AD-A128 034

DRSAR-LEP-L

AD

MEMORANDUM REPORT ARBRL-MR-03248

EXPERIMENTAL STUDIES OF MULTIDIMENSIONAL TWO-PHASE FLOW PROCESSES IN INTERIOR BALLISTICS

Thomas C. Minor

April 1983

US ARMY ARMAMENT RESEARCH AND DEVELOPMENT COMMAND
BALLISTIC RESEARCH LABORATORY
ABERDEEN PROVING GROUND, MARYLAND

UNCLASSIFIED

SECURITY CLASSIFICATION OF THIS PAGE (When Data Entered)

REPORT DOCUMENTATION PAGE		READ INSTRUCTIONS BEFORE COMPLETING FORM
1. REPORT NUMBER MEMORANDUM REPORT ARBRL-MR-03248	2. GOVT ACCESSION NO.	3. RECIPIENT'S CATALOG NUMBER
4. TITLE (and Subtitle) EXPERIMENTAL STUDIES OF MULTIDIMENSIONAL TWO-PHASE FLOW PROCESSES IN INTERIOR BALLISTICS		5. TYPE OF REPORT & PERIOD COVERED Memorandum Report Oct 80 - Sep 81
		6. PERFORMING ORG. REPORT NUMBER
7. AUTHOR(s) Thomas C. Minor		8. CONTRACT OR GRANT NUMBER(s)
9. PERFORMING ORGANIZATION NAME AND ADDRESS US Army Ballistic Research Laboratory ATTN: DRDAR-BLI Aberdeen Proving Ground, MD 21005		10. PROGRAM ELEMENT, PROJECT, TASK AREA & WORK UNIT NUMBERS 1L162618AH80
11. CONTROLLING OFFICE NAME AND ADDRESS US Army Armament Research & Development Command US Army Ballistic Research Laboratory (DRDAR-BLA-S) Aberdeen Proving Ground, MD 21005		12. REPORT DATE April 1983
		13. NUMBER OF PAGES 41
14. MONITORING AGENCY NAME & ADDRESS(if different from Controlling Office)		15. SECURITY CLASS. (of this report) Unclassified
		15a. DECLASSIFICATION/DOWNGRADING SCHEDULE
16. DISTRIBUTION STATEMENT (of this Report) Approved for public release; distribution unlimited.		
17. DISTRIBUTION STATEMENT (of the abstract entered in Block 20, if different from Report)		
18. SUPPLEMENTARY NOTES Presented at 18th JANNAF Combustion Meeting, Pasadena, CA, October 1981.		
19. KEY WORDS (Continue on reverse side if necessary and identify by block number) Interior Ballistics Flamespread Pressure Waves Stick Propellant Model Validation Propellant Temperature Interior Ballistics Models		

20. ABSTRACT (Continue on reverse side if necessary and identify by block number) dbl

The past few years have witnessed an increasing sophistication of two-phase flow interior ballistics models, including the advent of computer codes which consider more than one physical dimension. While the one-dimensional codes performed quite well in modeling ignition-induced phenomena in cased ammunition that approximates a one-dimensional propelling charge, they have enjoyed only a limited success, with uncompromised data bases, in predicting the performance of Army bagged charges, which exhibit multidimensional

DD FORM 1473 1 JAN 73 EDITION OF 1 NOV 65 IS OBSOLETE

UNCLASSIFIED

SECURITY CLASSIFICATION OF THIS PAGE (When Data Entered) characteristics both in loading configuration and in external constraints of the charge casing. With the coming of multidimensional treatment of the interior ballistic cycle, there then arises the need for experimental data to identify, and, where appropriate, to quantify the parameters of importance in multidimensional flow such as might be encountered in these bagged-charge situations.

This paper presents work conducted in the 155-mm interior ballistic simulator at the Ballistic Research Laboratory to produce such data. The simulator employed disposable chambers of plastic and fiberglass that permitted direct visualization, through high-speed photography, of gas- and solid-phase flow during the early portion of the interior ballistic cycle. Solid-phase dynamics were further monitored via flash radiography. In addition to breech and wall pressure measurements along the length of the chamber, data were obtained for some firings within the chamber and propellant bed for gas pressure and propellant heating using thermocouples mounted on grain surfaces. This investigation into multidimensional flow structure was carried out through examination of the ignition portion of the cycle of several charge types: stick and granular charges of M30A1 propellant loaded in a one-dimensional configuration, to investigate the pressurization and flamespread in each; multiple-increment charges with varying chamber atmosphere and igniter, to study gas-phase combustion; and an M203-type charge, to investigate internal charge pressurization and heat transfer to the propellant.

TABLE OF CONTENTS

LIST OF ILLUSTRATIONS

LIST OF ILLUSTRATIONS (Cont.)

I. INTRODUCTION

A. PROPELLING CHARGE PHENOMENOLOGY

In this paper several aspects of the multidimensional two-phase flow in the early portions of the gun interior ballistic cycle are examined. The two-phase flow character of ignition and flamespread has been described on many occasions; it is briefly recounted here, with reference to Figure 1. An igniter stimulus, whose intensity and distribution are system dependent, is applied to the propellant, venting hot combustion gases into the bed. These gases heat neighboring propellant grains to ignition, and the gases from this combustion join those of the igniter to produce a convectively driven ignition wave, resulting in flamespread through the charge. The packed propellant presents resistance to the flow of these gases, which can lead to large pressure gradients within the charge, and perhaps even induce substantial movement of the propellant. Especially in charges ignited at the base with ullage concentrated at the forward end of the charge, considerable velocities can be attained by the solid phase. Stagnation at the projectile base then may be accompanied by high local pressurization, leading to the formulation of traveling axial pressure waves, and perhaps even grain fracture.

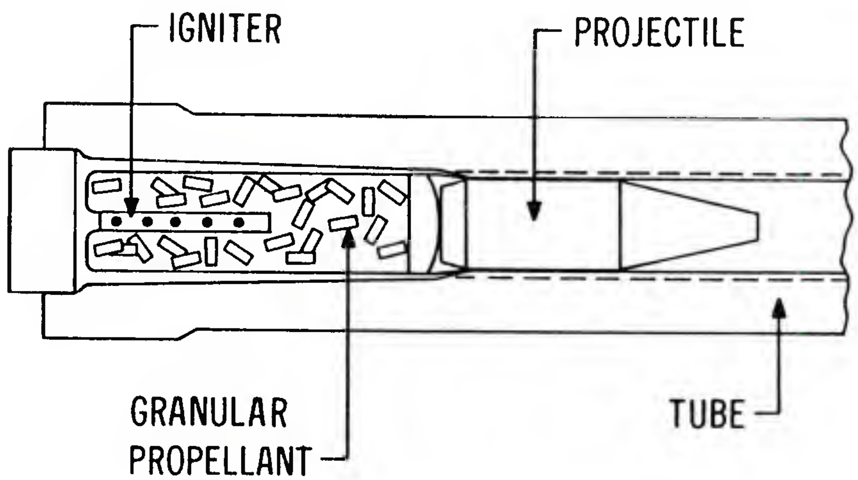

Figure 1. Schematic of Gun Propelling Charge

Even in this idealized, one-dimensional view of ignition and flamespread, it is not difficult to see how the effects of drag offered by a packed propellant bed can be mitigated by the introduction of stick propellant. The natural channels produced by bundled stick propellant drastically increase the permeability of the propellant bed, allowing relatively easier passage of igniter and early propellant gases to other axial regions of the charge. In response to base ignition, rapid flamespread throughout the charge would be expected, since the entire length of the charge would be quickly bathed in igniter gases. And since the stick propellant offers less drag on igniter and propellant gases, there should not be much movement of the propellant itself. The manifestation of these phenomena in the past has been in reduced axial pressure waves, rather than in direct evidence of the functioning of a stick charge.[1]

Some of the multidimensional aspects of the gun interior ballistic cycle are perhaps best illustrated with reference to Figures 2 and 3, which depict typical examples of bagged Army artillery propelling charges. One type, schematically illustrated in Figure 2, consists of a single increment, packaged in a bag, and is centercore-ignited. The intended mode of ignition for this charge entails a discharge of hot gases from the primer onto a basepad, which then burns and serves as an ignition transfer to a pouch (the "snake") of black powder contained within the nitrocellulose centercore igniter tube. Rapid flame propagation through the snake and centercore, with its radial venting of hot gases, should then assure uniform axial ignition of the charge. In reality though, the charge is undersized with respect to the internal dimensions of the chamber, creating ullage radially, in front of the charge, and between the spindle and charge (standoff). This allows for a variety of complex flows depending upon the initial loading configuration. The centercore tube does not necessarily align with the primer output upon loading, reducing the efficiency of ignition transfer from primer to centercore. The profile of heat[2] and particulate output in the vicinity of the basepad and centercore is a complex one, both in space and intensity, and the burning basepad may locally ignite propellant grains at the rear of the charge, producing a competition between ignition of the charge by the centercore or by locally burning propellant at the base of the charge. The charge casing, a fabric bag with lead and wear-reducing liners attached at various points along its length, is of grossly nonuniform strength and permeability. Gases may pass through it at some points more easily than at others, and pressure differentials within the bag and between the bag and ullage may produce complex movement of propellant, rupture of the bag, and the like.

The multidimensional and physical complexity of Army bagged artillery charges is perhaps even more strongly pronounced in a multi-increment charge, as shown in Figure 3. This charge consists of several bags of propellant tied together, with a basepad serving as the sole ignition stimulus. This type of charge is generally even more undersized with respect to chamber dimensions than is the single-bag charge, creating more radial ullage for venting of early combustion products toward the front of the chamber. Parasitic components attached to and embedded within the charge may serve to block the passage of igniter and propellant gases. A multiple-increment charge may have more than one granulation propellant, and the localized ignition and brisant combustion of a fine-web, base-increment

[1] A. W. Horst and T. C. Minor, "Improved Flow Dynamics in Guns Through the Use of Alternative Propellant Grain Geometries," 1980 JANNAF Propulsion Meeting, CPIA Publication 315, Vol. I, pp. 325-351, March 1980.

[2] E. B. Fisher, "Continued Investigation of Early Time Propellant Charge Behavior," Report No. 6816-D-1, Calspan Corporation, Buffalo, NY, June 1981.

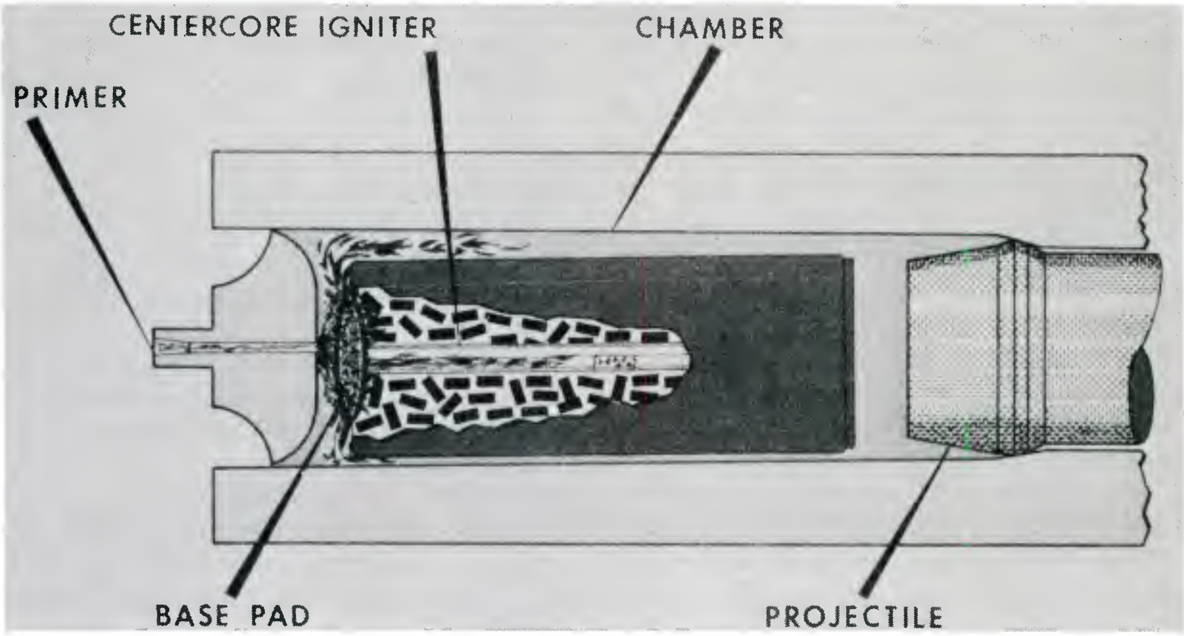

Figure 2. Phenomenology, Single-Increment, Bagged Artillery Charge

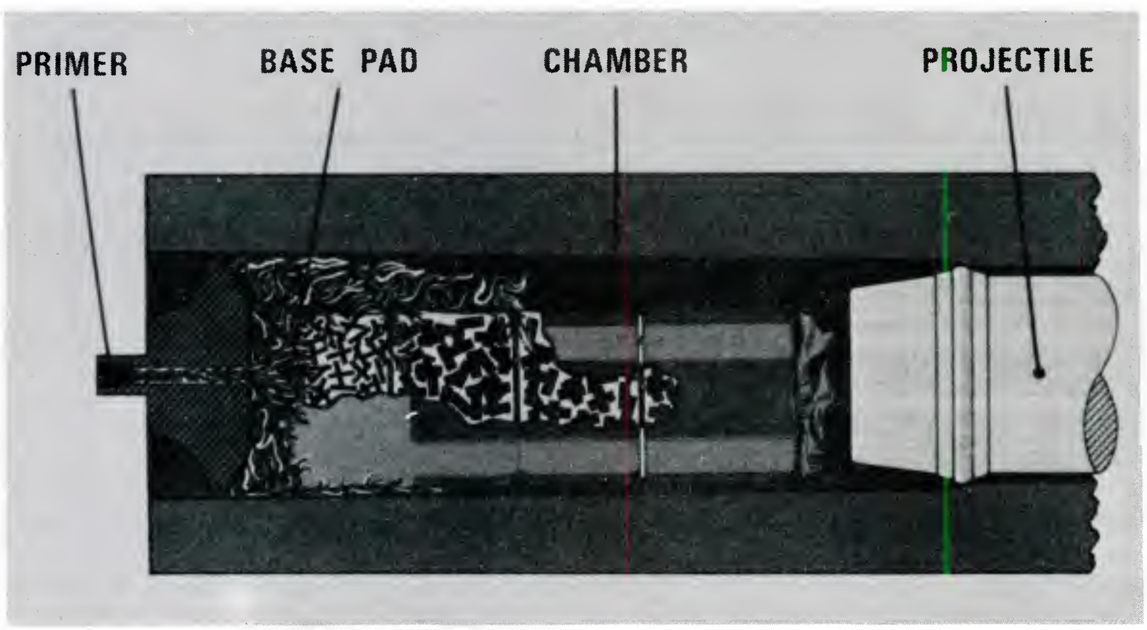

Figure 3. Phenomenology, Multiple-Increment, Bagged Artillery Charge

propellant may induce pressure waves and perhaps even considerable movement of relatively massive, entire packages of propellant. Several distinctive phenomena associated with this type of charge have been previously reported.[3] Igniter gases were seen to flow through the radial ullage, with several acoustic oscillations along the chamber. Later, a very intense, possible gas-phase combustion was observed at the forward end of the chamber, and separation and movement of the forward charge bag at high velocity was observed.

B. SCOPE OF THE INVESTIGATION

The results of several studies to investigate some of the multi-dimensional and multiregional related aspects of the early interior ballistic cycle are presented here. Specifically addressed are flamespread, chamber pressurization and solid-phase movement in one-dimensional, stick and granular propellant charges. Also described are the results of further experiments with multi-increment charges to investigate flow of gases through radial ullage, gas-phase combustion, and propellant movement. Lastly, a discussion of our first experiments to measure pressure and propellant temperature within an Army artillery propelling charge is given.

II. EXPERIMENTAL

A. APPARATUS

The apparatus used to conduct the studies described here is shown in Figures 4 and 5. The massive mount, constructed of armor plate, accepted either plastic chambers (Figure 4) or axially reinforced, filament-wound fiberglass chambers (Figure 5). The plastic chambers were commercially available, cast acrylic tubing with nominal inner and outer diameters of 165 mm and 191 mm, respectively. The clear plastic offered much better visibility of the events transpiring within than did the fiberglass, but it fractured at significantly lower pressures. The pressure limit for these tubes was found to be variable from sample to sample and was pressure-rise-rate dependent. The fiberglass chambers were manufactured by the Naval Surface Weapons Center, Dahlgren, VA, and were wound on a mandrel to the interior dimensions of the 155-mm, M199 cannon chamber. The chambers were wound in a near-hoop mode, with occasional layers of a fiberglass/epoxy fabric sheet for axial strength, to a finished thickness of approximately 3-4 mm. After curing, a steel plate bearing Kistler gage ports was attached with sufficient fiberglass wraps to hold it in place, and holes were drilled from the adapters through the chamber wall. For all the chambers the muzzle end of the chamber was closed by a projectile seated in a section of gun tube machined to the dimensions of the M199. The breech end of the apparatus was closed by an M185-type spindle with centrally aligned spithole. As Figure 6 shows, the spindle accepted three Kistler 607C piezoelectric pressure transducers, and an array of five additional pressure gages could be mounted on the fiberglass chamber sidewall along its axis.

[3] T. C. Minor, "Characterization of Ignition Systems for Bagged Artillery Charges," 17th JANNAF Combustion Meeting, CPIA Publication 329, Vol. II, pp. 45-67, November 1980.

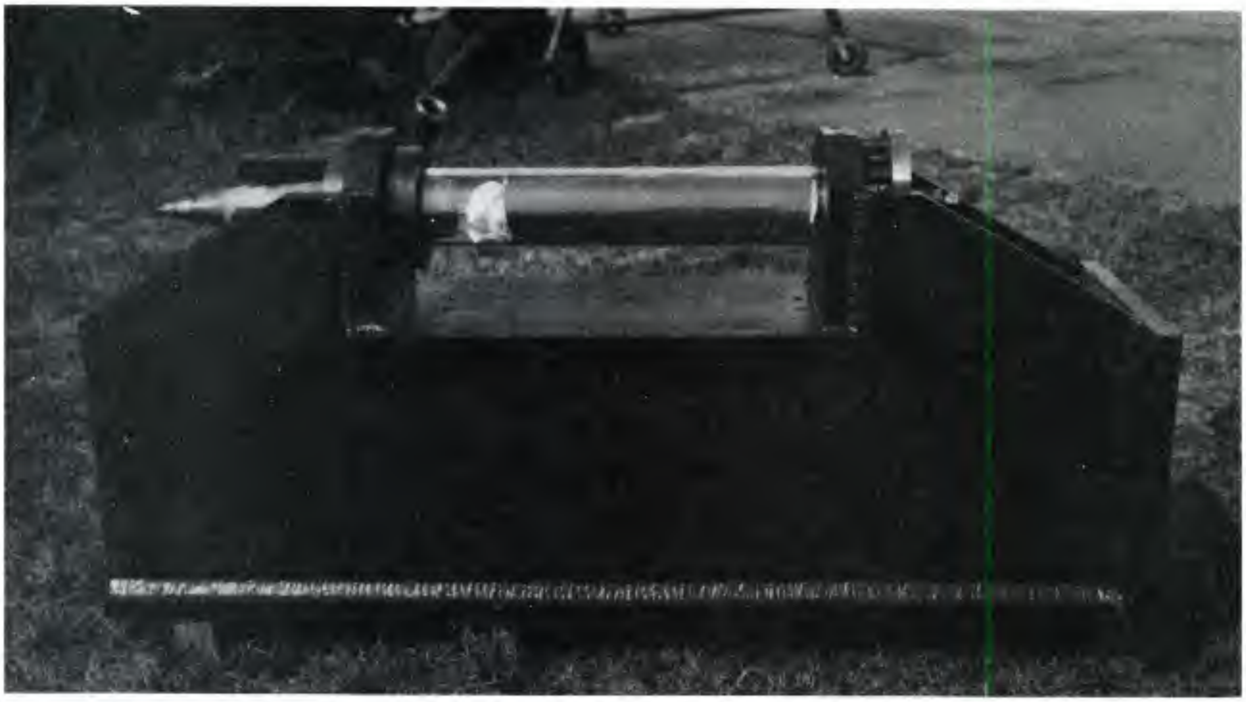

Figure 4. 155-mm Simulator, Plastic Chamber

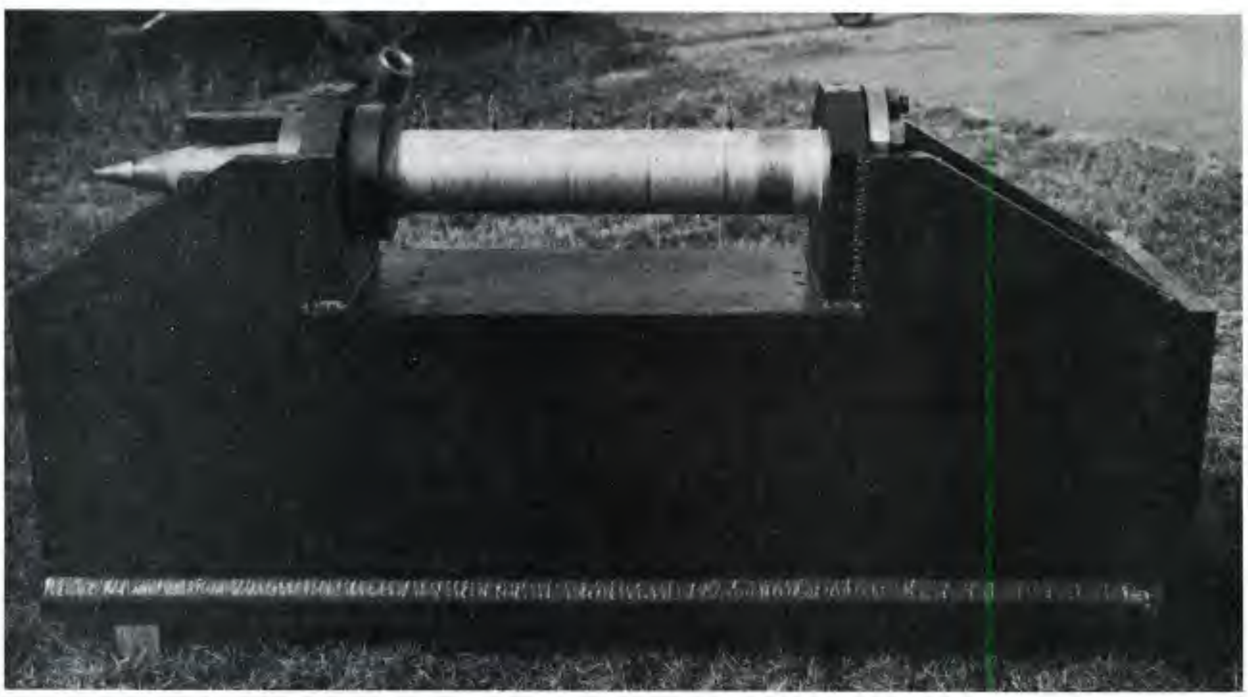

Figure 5. 155-mm Simulator, Fiberglass Chamber

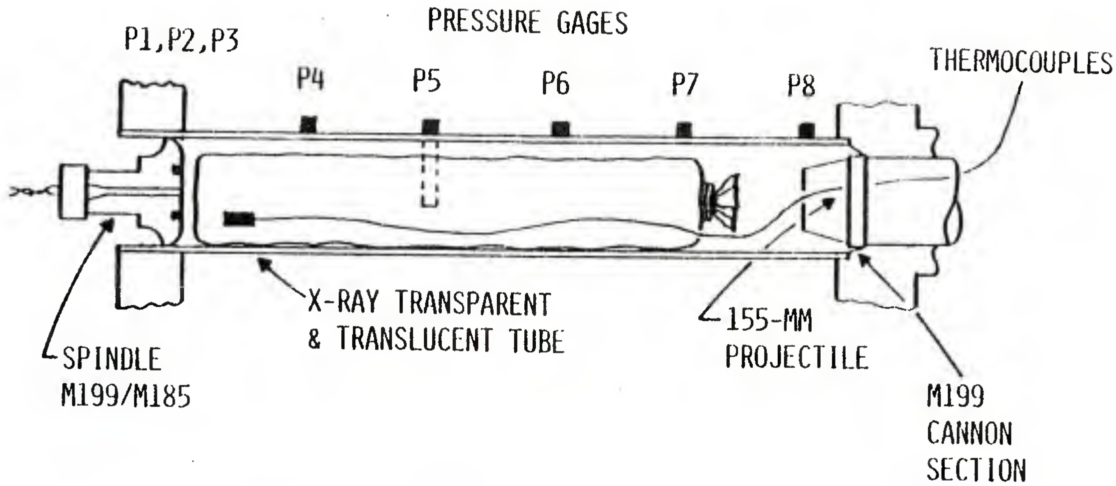

Figure 6. Schematic of 155-mm Howitzer Simulator

A change in the apparatus from earlier investigations[3] was introduction of transducers into the propelling charge itself. Provisions were made to extend the pressure gage holders inside the chamber, using low-pressure, O-ring seals at the chamber wall. This permitted direct measurement of pressure within the propelling charge at any of the positions P4 . . . P8, at selectable radial depths within the propelling charge. Propellant grains instrumented with thermocouples were placed within the charge, and the signal wires brought out through the projectile base.

Photographic data were recorded with a Hycam 40, high-speed, 16-mm camera. For the tests reported here, the data were recorded on Kodak Ektachrome 7241 film at a framing rate of approximately 5000 pictures per second. A 1-kHz timing signal was placed on the film by electronics internal to the camera, and the firing fiducial (time at which the firing voltage is applied to the gun) was also recorded on the film to aid in correlation of the film data with other data. For some of the tests, a mirror was positioned behind the mount to allow simultaneous recording on a single frame of events occuring on both sides of the chamber.

Flash X-rays were used on some of the tests to monitor the movement of the solid phase. A total of four, 300-kV X-ray heads was used, two at one axial location, separated by approximately twenty degrees (Figure 7), and another two at a further axial location, similarly separated, to cover the length of the tube. The overlapping images from the two sets of heads were recorded on a single sheet of film, yet it was possible to determine the X-ray source of each image. One image was created by X-rays triggered by movement of the propellant bed, as determined by a break circuit inserted into the tube, and the second image was made by the X-ray heads triggered at a predetermined time delay after the first. Particular grains in the propellant bed were identified by small steel cylinders embedded within them. The combination of seeded grains and radiographic images of known time separation allowed measurement of an average velocity of the propellant bed. The radiographs were recorded on Kodak XR-5 film using Dupont Lightning Plus intensifier screens. The film was protected from the blast of the disposable chamber by a wooden cassette, with the forward face composed of layers of air spaces and sacrificial wooden plates.

Figure 7 depicts the system for experiment control, data acquisition, and data reduction. The Ballistic Data Acquisition System (BALDAS) performed these tasks, driven by a PDP 11/45 minicomputer. By starting a programmed sequence timer, BALDAS controlled the firing of the high-speed camera and enabled an X-ray trigger circuit. At the appropriate time, BALDAS exercised an in-line, five-step, calibration for each data channel, then fired the cannon and acquired and digitized analog data through a 16-channel, 10-bit, 24-K word analog-to-digital converter. At the same time, a backup analog record was made on a 14-channel FM tape recorder. BALDAS-resident digital counters recorded the time of the firing fiducial and other events, such as X-ray trigger pulses. After the data were acquired, BALDAS calibrated the data via a second-order, least-squares fit to the calibration staircase, and then reduced the data, through suitably introduced gage constants.

B. CHARGE DESIGN

A schematic of the one-dimensional, M30A1 propelling charges is shown in Figure 8. The charges were made to full-chamber diameter and loaded in an aluminum screen bag, to allow unobstructed visualization of the flame within the charge. The charges were ignited with 142 g of Class 1 black powder. The black powder basepad was spread out as uniformly as possible over the base of the charge in an attempt to produce a planar ignition stimulus. The granular charge was made from propellant lot RAD-79E-069960, and had a mass of 15.30 kg. The propellant cylinders were seven-perforated, with a length of 24.3 mm and an outer diameter of 10.5 mm. The stick charge was made from lot RAD-PE-480-55, and had a mass of 17.23 kg. These single-perforation, unslotted sticks had a length of 737 mm and an outer diameter

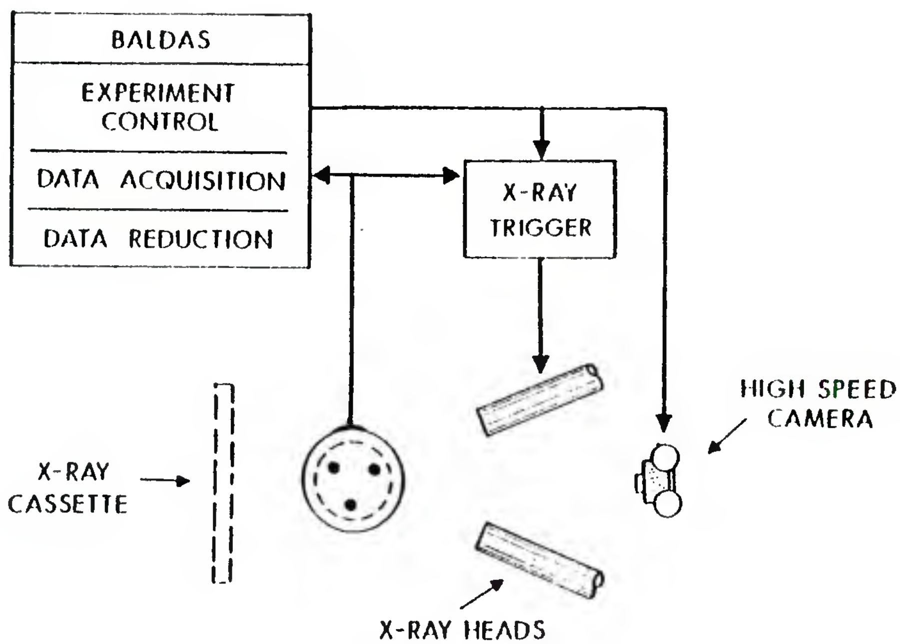

Figure 7. Instrumentation, Experiment Control, and Data Acquisition for 155-mm Howitzer Simulator.

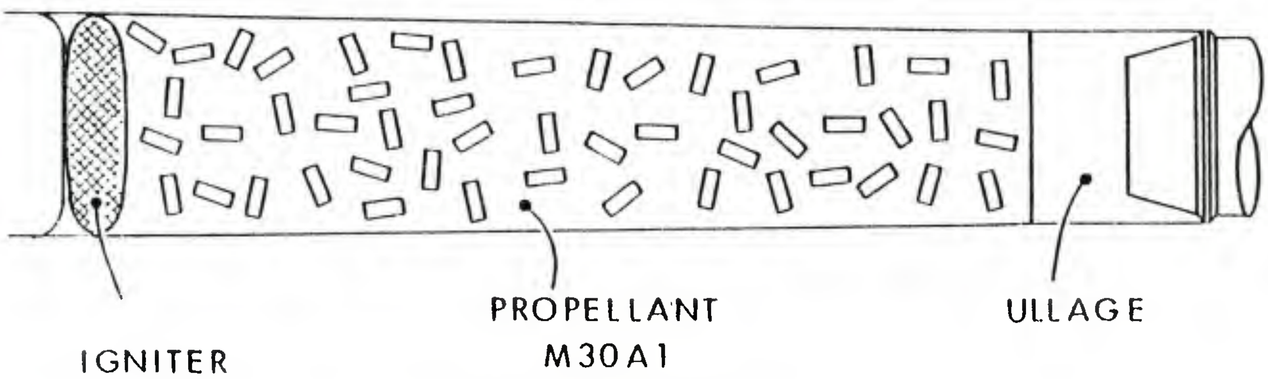

Figure 8. Charge Schematic, One-Dimensional Charge Tests

of 7.3 mm. The finished length of the charges was approximately 750 mm, which left some axial ullage between the forward end of the charge and the projectile base. This ullage was employed to allow some movement of the charge before the X-ray trigger circuit was activated. As described earlier, several seeded grains were placed throughout the granular charge to assist in interpreting the flash radiographs.

A schematic of the multizone charges fired in these tests is shown in Figure 9. This charge, based on the 155-mm, XM211, development of which has been terminated, is identical to that fired in an earlier study[3] that showed separation and acceleration of the forward charge increment, and possible gas-phase combustion of igniter and pyrolized propellant products at the forward end of the chamber. Only Zone 5 charges were fired in this study. The base increment, Zone 3, consisted of 1.67 kg of 0.33-mm, single-perforation, M1 propellant. Zones 4 and 5 contained, respectively, 0.79 and 1.45 kg of 0.97-mm, M1, seven-perforation propellant. The baseline charge

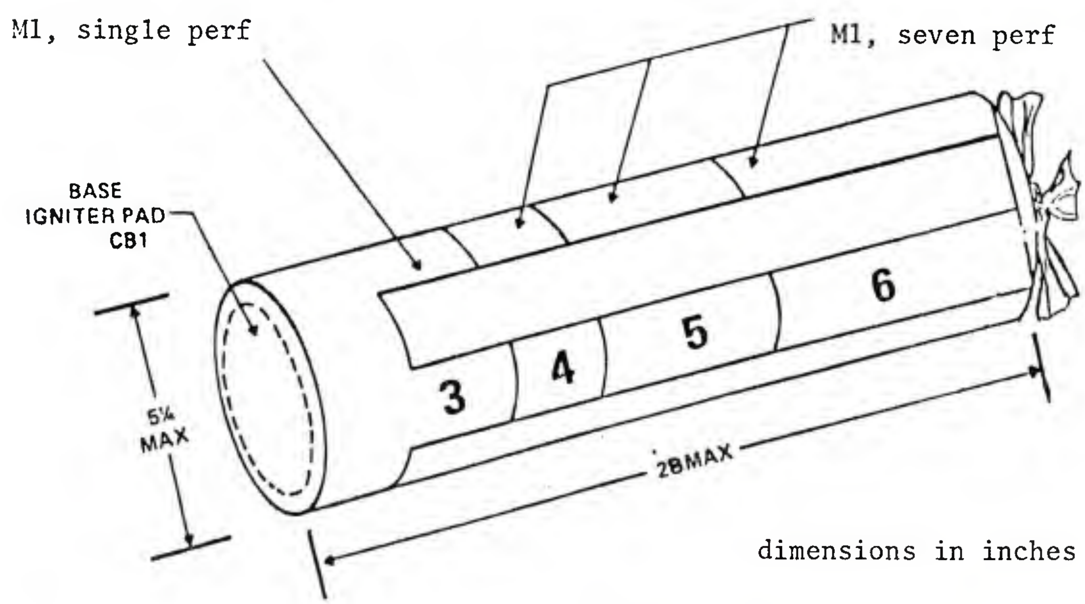

Figure 9. Charge Schematic, Multi-Zone Charge Tests

was ignited with an 85-g basepad of Clean Burning Igniter (CBI). Another baseline charge was fabricated, to be fired in a chamber purged with nitrogen, in order to assess the effect of available oxygen on the combustion. To investigate the effect of igniter composition on early gas-phase combustion, a second charge with an 85-g basepad of Class 5 black powder was fabricated.

A photograph of the 155-mm, M203 charge used to investigate propellant grain temperatures within the charge and pressures within and without the charge is shown in Figure 10. Figure 11 is a schematic depicting modifications to the charge for the experiments. Two charges were made, one to monitor the pressure inside the charge in the region where the casing consisted of only fabric, and one in the region surrounded by fabric, lead foil, and wear-reducing liner. A pouch, 38 mm in diameter and 32 mm in depth, and in each case made of the casing materials of the region, was sewn into the bag sidewall to allow introduction of the gage holder into the charge. A hole was cut in the casing material at the bottom of the pouch to permit the pressure gage to be placed directly inside the propellant bed. Four thermocouple-instrumented grains were placed in each charge. The locations of pressure transducers and thermocouples in each of the two charges are given in Figure 12.

Figure 13 portrays a thermocouple-instrumented propellant grain. The thermocouple, a butt-welded, 0.005-mm thick chromel-alumel junction, was attached with acetone to a flat surface of a live M30A1 propellant grain, from which the graphite coating had been removed. Care was taken that the junction was not placed over a perforation. The thermocouple leads were glued to the side of the grain, again with acetone, and were attached to fine copper wires at the base of the grain. The copper-alumel and copper-chromel junctions were protected with a thermal jacket of fiberglass and aluminum foil. A heat source that produced a response of the thermocouple and ignited the propellant grain produced only an 80-microvolt (2°C) response when directed at the protected area.

III. RESULTS AND DISCUSSION

A. ONE-DIMENSIONAL CHARGE TESTS

The one-dimensional, full-bore charges were fired in fiberglass chambers. There was no charge standoff, and M82 primers were used to initiate the charges. The charges were conditioned to 21°C before firing. Figures 14 and 15 present, respectively, the chamber pressures from the one-dimensional, M30A1, granular and unslotted-stick charges. Figures 16 and 17 display portions of the flamespread data from these same tests. The key to the pressure traces can be obtained from Figure 6; each gage was separated from its neighbor by 165 mm. The times are referenced to the instant at which the firing voltage was applied to the cannon. In the photographs, the breech is at the bottom and the projectile at the top.

The progression of the pressure front through the packed granular propellant bed is clearly seen in Figure 14. The tube fractured before any wave reflected by the projectile base passed any of the sidewall gage positions. The first discernible luminosity at the spindle was not seen until approximately 7.2 ms after application of the firing voltage, and

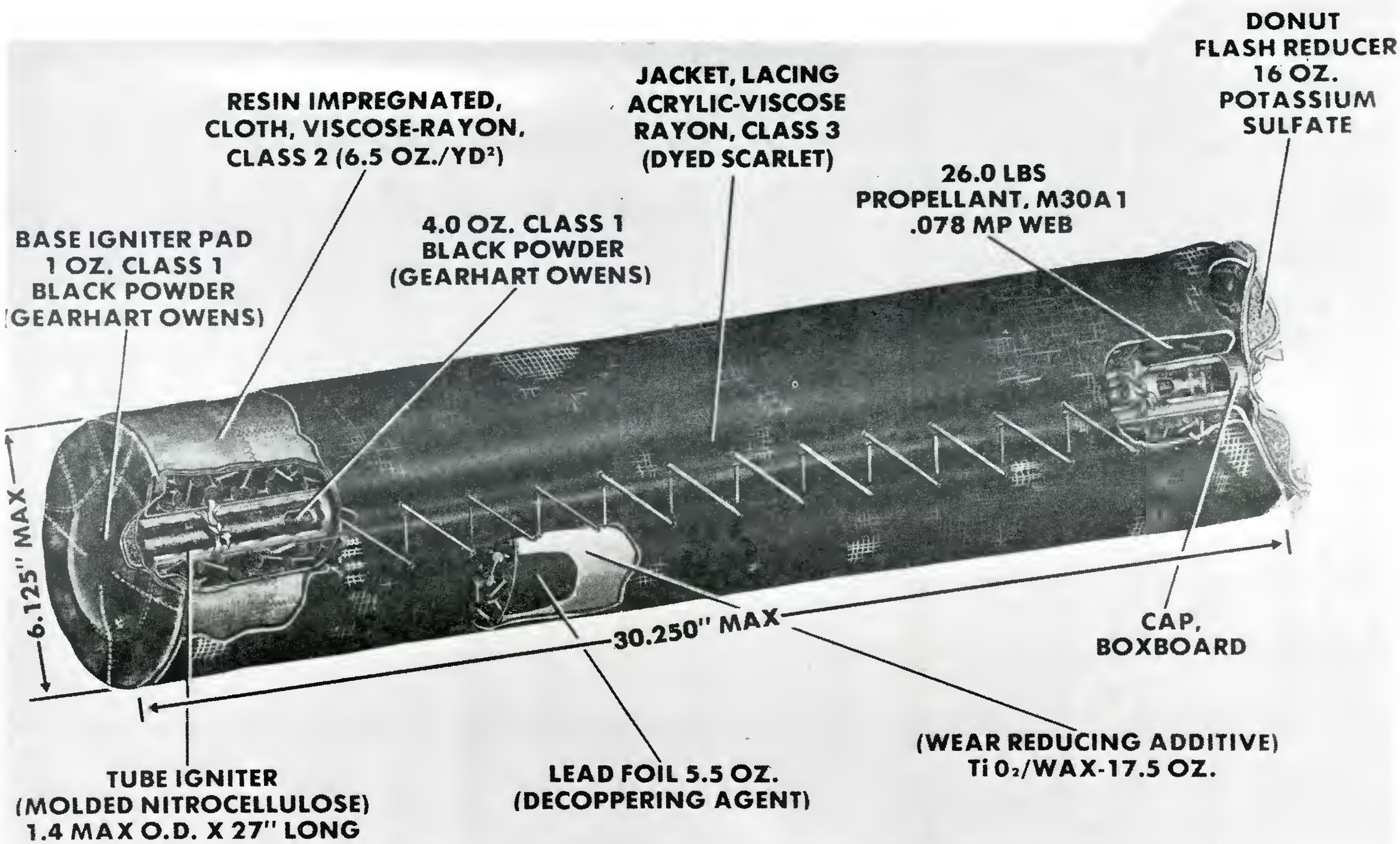

Figure 10. 155-mm, M203 Propelling Charge

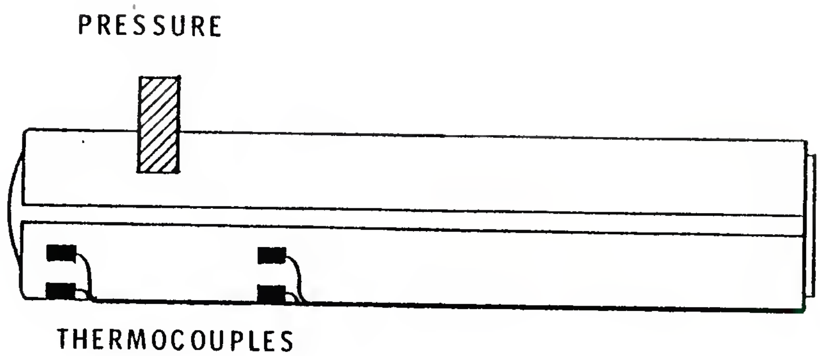

Figure 11. Charge Schematic, Instrumented M203 Propelling Charges

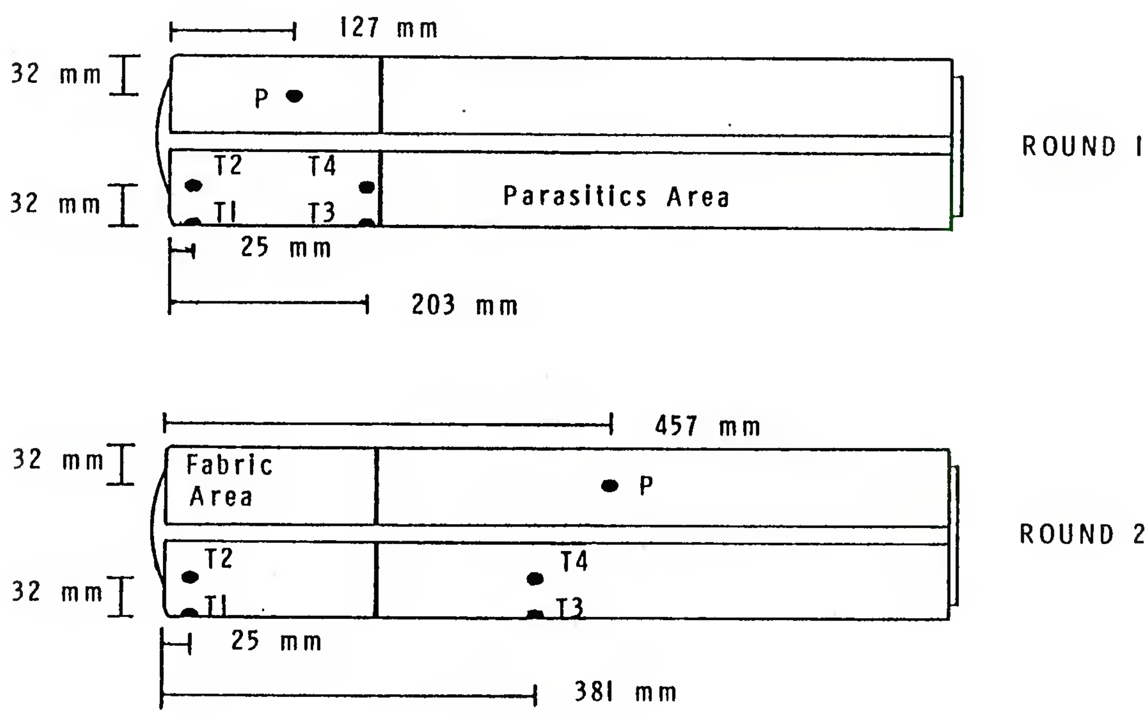

Figure 12. Locations of Pressure and Temperature Transducers in M203 Charges

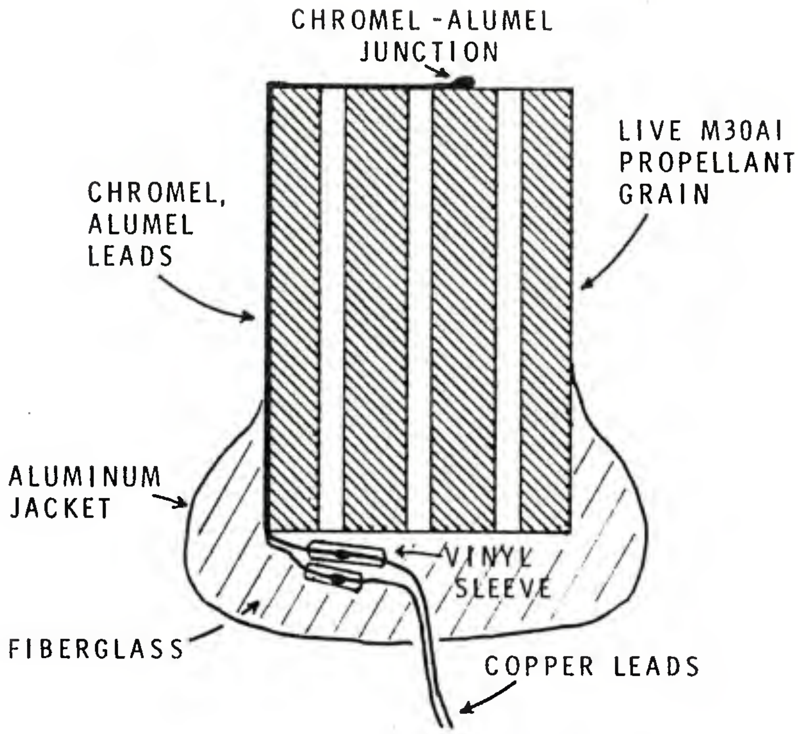

Figure 13. Thermocouple-Instrumented M30A1 Propellant Grain

though the base area continued to burn after this time, there was no obvious movement of the flamefront into the propellant bed until approximately 13.6 ms. The record of the flamespread through the charge was difficult to read, due to the lack of a well-defined front, but the forward-most reaches of the flame could be located at several later times.

The ease with which igniter gases and the products of early propellant combustion pass through the stick propellant charge is illustrated in both Figure 15 and Figure 17. The delay between pressurization of the breech and forward ends of the case is substantially less with the stick charge than with the granular. The evidence is even more striking in the flamespread photographs, displayed in Figure 17. First light from the base region of the charge was seen at 6.2 ms after application of the firing voltage to the cannon. The base region continued to burn, and at 8.0 ms there was considerable luminosity only at the base, with light nowhere else within the chamber. At 8.4 ms, faint luminosity was seen at the forward end of the chamber; it became more intense by 8.6 ms, due to stagnation of igniter gases and early combustion products at the projectile base. Before 9.0 ms, no luminosity was seen along the length of the charge; at this time flame appeared throughout the chamber, outlining the propellant sticks. The luminosity continued to increase uniformly throughout the charge until the chamber fractured at 9.8 ms.

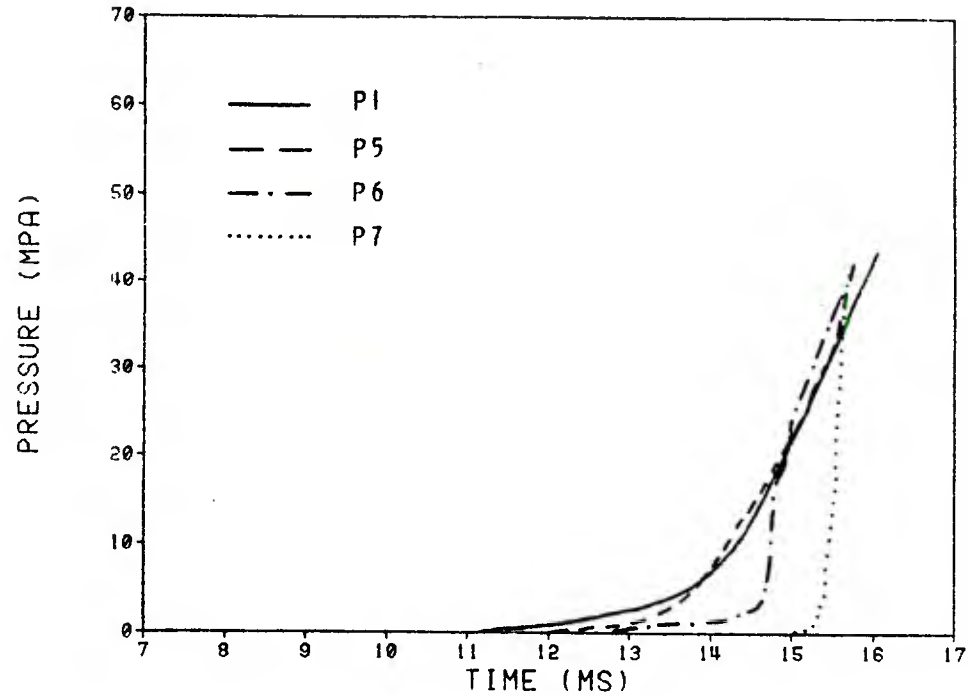

Figure 14. Chamber Pressures, One-Dimensional, Granular Charge

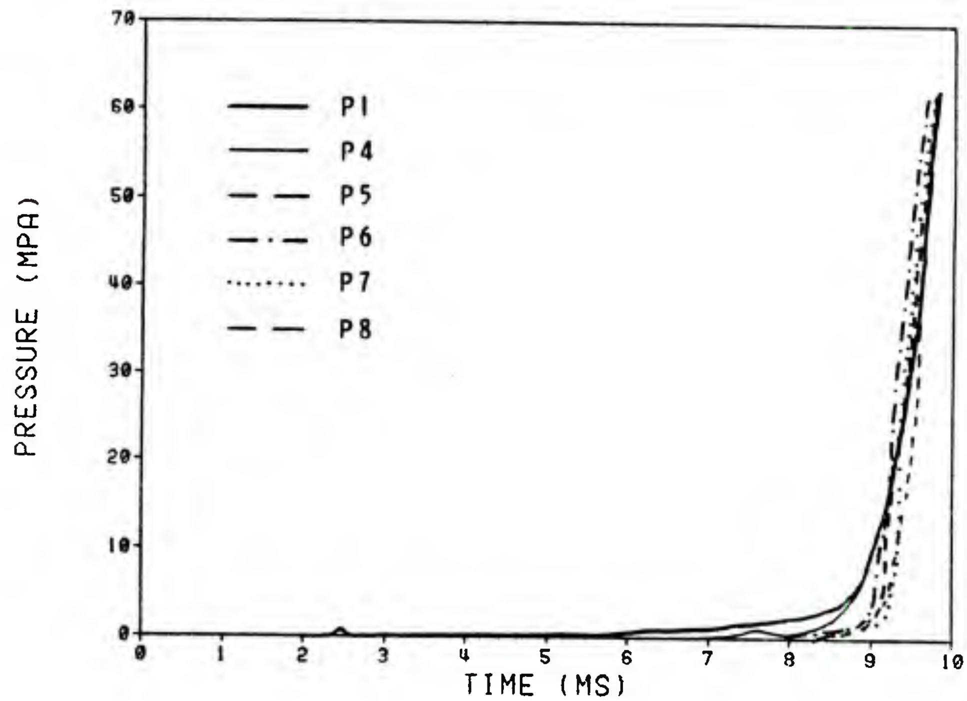

Figure 15. Chamber Pressures, One-Dimensional, Stick Charge

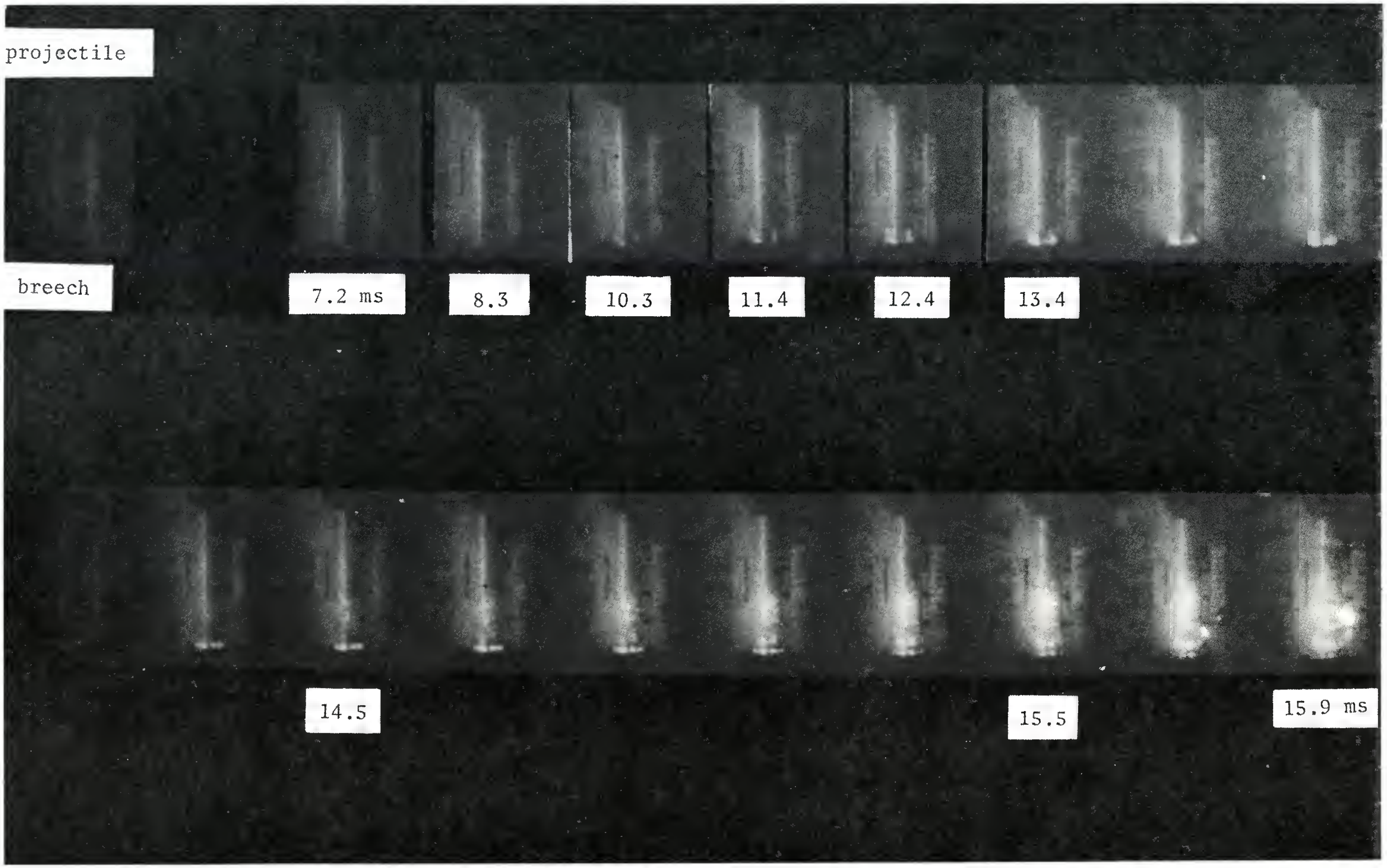

Figure 16. Flamespread, One-Dimensional, Granular Charge

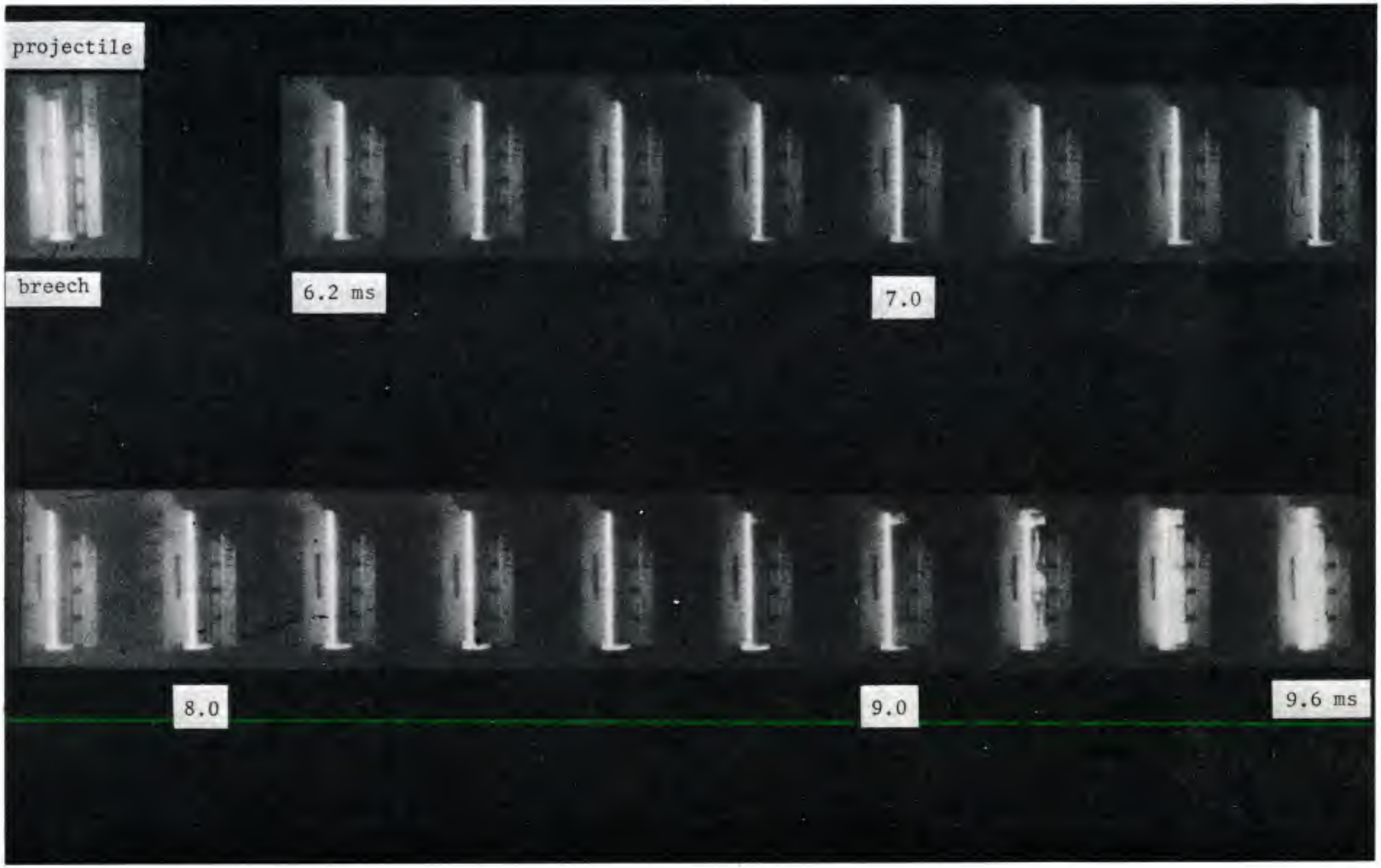

Figure 17. Flamespread, One-Dimensional, Stick Charge

Flash X-rays were used to monitor movement of the solid and granular stick propellants. The average velocity of the granular propellant before impact on the projectile base was on the order of 60 m/s. While the X-rays recorded no movement of the stick propellant up to a base pressure of 7 MPa, a witness plate attached to the projectile base showed that some of the grains from the center of the charge impacted the projectile.

B. MULTIZONE CHARGE TESTS

Each of the three multizone charges was fired in an acrylic chamber with a charge standoff of 25 mm. Portions of the high-speed photography data are displayed in Figure 18 and pressure-time records are shown in Figure 19 for each of the following shots:

Multizone Round 1 - Zone 5 charge, 85-g CBI basepad, ambient chamber atomsphere

Multizone Round 2 - Zone 5 charge, 85-g Class 5 black powder basepad, ambient chamber atmosphere

Multizone Round 3 - Zone 5 charge, 85-g CBI basepad, nitrogen chamber atmosphere.

The results from Round 1 mostly reproduced those reported earlier.[3] After initiation by the primer, the basepad began to burn. Concurrent with this combustion were several acoustic oscillations of a small luminous front in the radial ullage. As the cycle proceeded, there was a very strong luminosity at the forward end of the chamber before any substantial burning of the base region of the charge proper. Again, this phenomenon was probably due to gas-phase combustion of products pyrolized from the igniter and propellant early in the cycle. The charge proper then began to burn, and the plastic tube fractured. Though this was a repeat of tests we reported earlier, and to a large degree reproduced the earlier results, it is important to note one substantial difference. The forward, Zone 5 increment detached from the package and was propelled toward the projectile at a velocity of about 150 m/s in the earlier test. No such separation and movement was noted here.

Round 2 displayed the same very early behavior as seen in Round 1, with the oscillation of the primer pulse in the ullage. There was some combustion in the forward area of the chamber prior to the obvious burning of the rear of the charge, but the luminous intensity was not nearly as great. Round 3, a repeat of the baseline charge with a nitrogen atmosphere, was markedly different from Round 1. The primer pulse and its oscillations were not nearly as pronounced as with the baseline case, and there was almost a total lack of any combustion in the forward portion of the chamber until the rear of the charge proper began to burn. As with the previous rounds, the charge did not move measurably.

A great deal of the difference in the luminous intensity between Round 1 and Round 2 can probably be attributed to the difference in the flame temperatures of CBI and black powder. Yet other factors could combine to produce the same result. The output from CBI is clean and gaseous, while

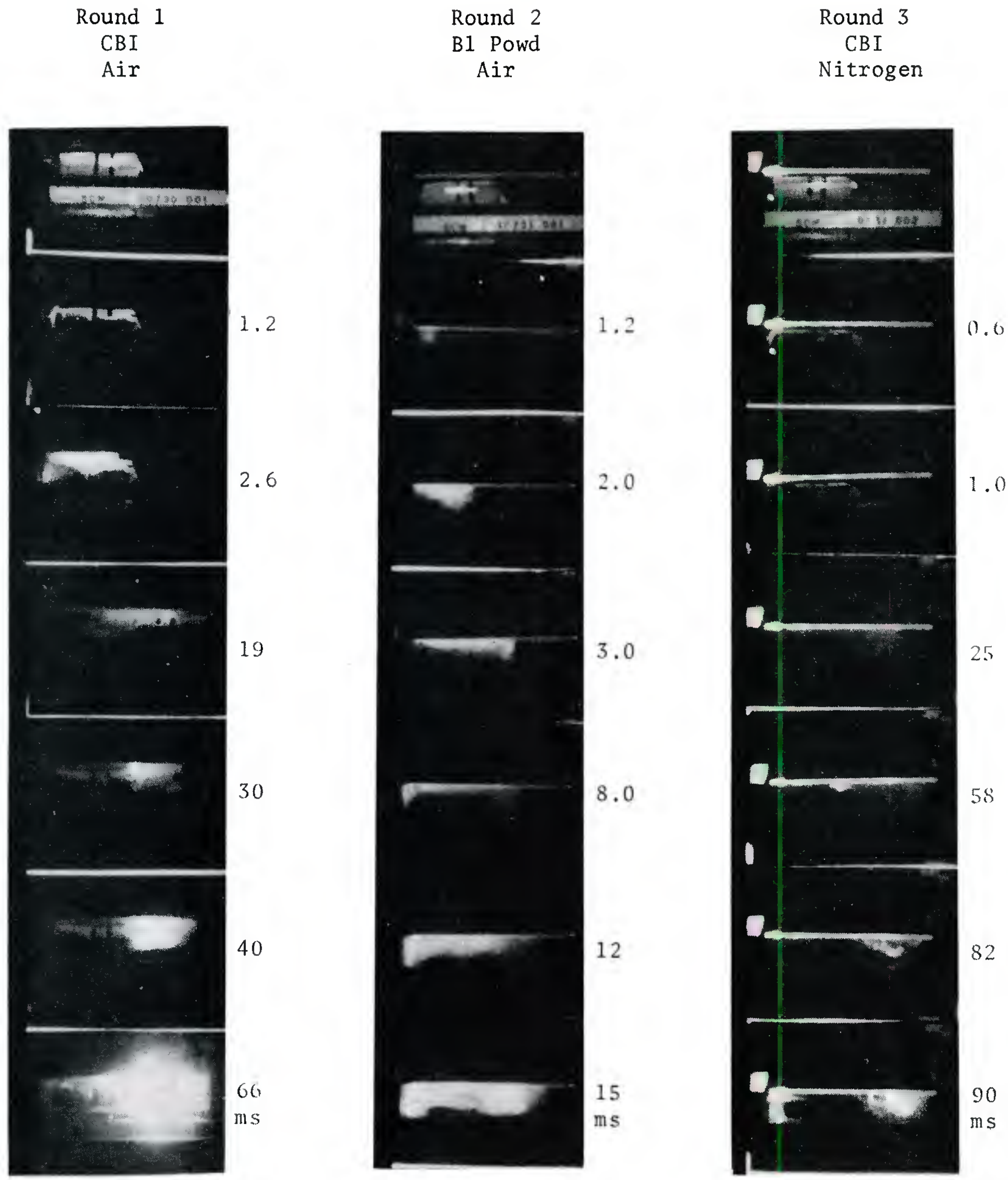

breech is on the left in each frame

Figure 18. Flamespread, Multizone Charges

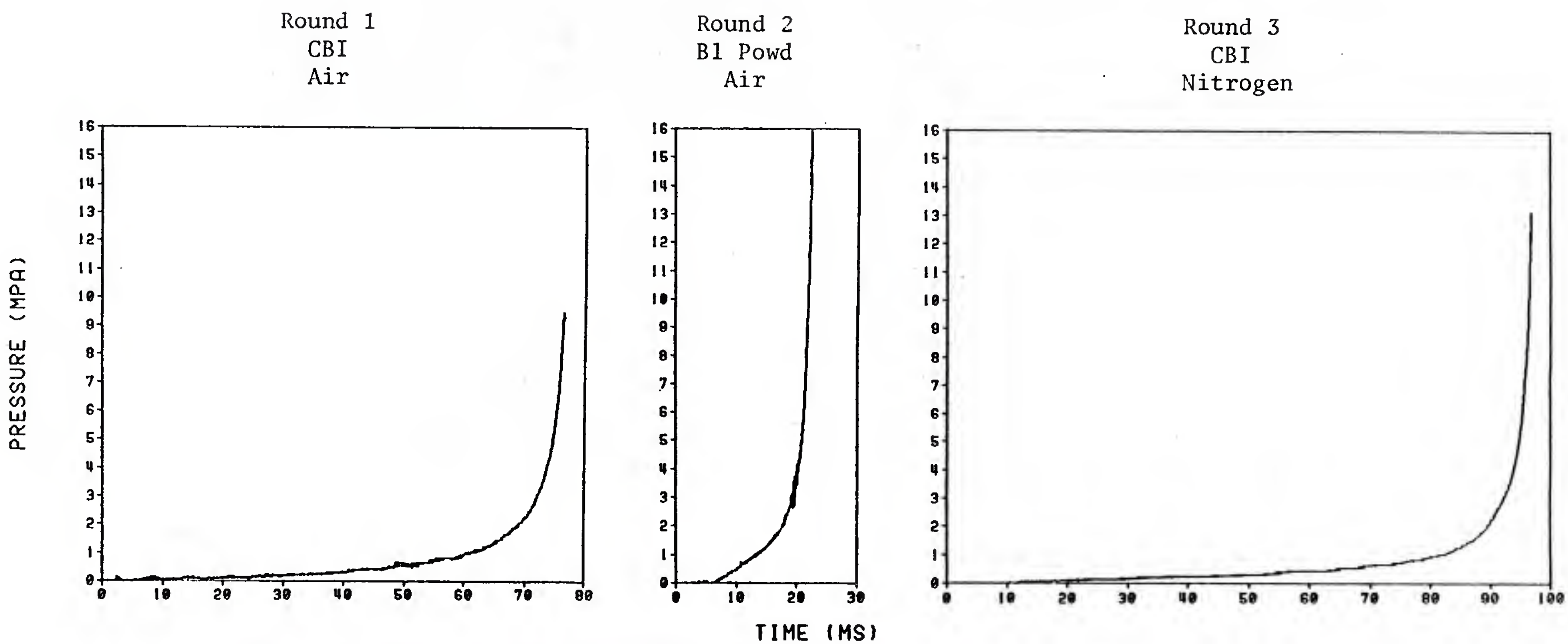

Figure 19. Pressure-Time Curves, Multizone Charges

that from black powder is much dirtier with a substantial amount of particulate. These black powder products are optically dense, so that much of the luminous output is prevented from escaping the chamber. In addition, the large amount of heat-absorbing surface area within the chamber might tend to cool the lower-temperature black powder gases to less luminosity more quickly than the hotter CBI gases. The oxygen in a chamber filled with propellant has no real significance in high-pressure combustion since the small amount available is consumed rapidly. A comparison of the results of Rounds 1 and 3 demonstrates, however, the significance of the oxygen at low pressures (<2MPa). In place of the very intense gas-phase burning of Round 1, there was essentially no early gas-phase combustion in Round 3.

C. M203 CHARGE TESTS

The results of the multidimensional, or perhaps more correct, multi-regional, tests with M203 Propelling Charges are presented in Figures 20-25. The charges were fired in the 165-mm diameter cast acrylic chambers with a standoff of 25 mm. The charges were supported in the chamber to make the loading configuration axisymmetric, and since the average diameter of the charges was approximately 145 mm, there was a radial distance of about 10 mm between the chamber wall and charge. The charges were fired at an ambient temperature of about 27°C. They were initiated with M82 primers.

Figure 20 presents a comparison of pressure measured in the ullage with that recorded inside the propellant bed in the region where the charge casing is solely fabric. At this scale, the pressure traces essentially overlay one another; an examination of the digital records of the event at several points shows no difference greater than 0.15 MPa until the plastic tube failed at 4.5 MPa, with the pressure in the ullage being slightly higher than that within the bed. Whether this measured difference is experimentally significant is questionable, given the noise of the traces and the lack of an absolute, side-by-side calibration of the gages. The lesson here is that the bag fabric and radial porosity discontinuity do not support large pressure differences in this pressure regime. It should be noted that calculations with a two-phase flow, two-dimensional axisymmetric interior ballistics code have shown no significant pressure difference between these two regions.[4,5]

Figure 21 depicts the temperatures measured at 25 mm from the base of the charge at two radial locations, and Figure 22 shows temperatures measured at the two radial positions at a distance of 203 mm from the base. As Figure 12 illustrates, these sensors are within the region of fabric only.

---

[4] P. S. Gough, "Two-Dimensional Model of the Interior Ballistics of Bag Charges," 18th JANNAF Combustion Meeting, CPIA Publication 347, Vol. II, pp. 193-199, October 1981.

[5] A. W. Horst, F. W. Robbins and P. S. Gough, "A Two-Dimensional, Two-Phase Flow Simulation of Ignition, Flamespread, and Pressure-Wave Phenomena in the 155-mm Howitzer," 18th JANNAF Combustion Meeting, CPIA Publication 347, Vol. II, pp. 201-215, October 1981.

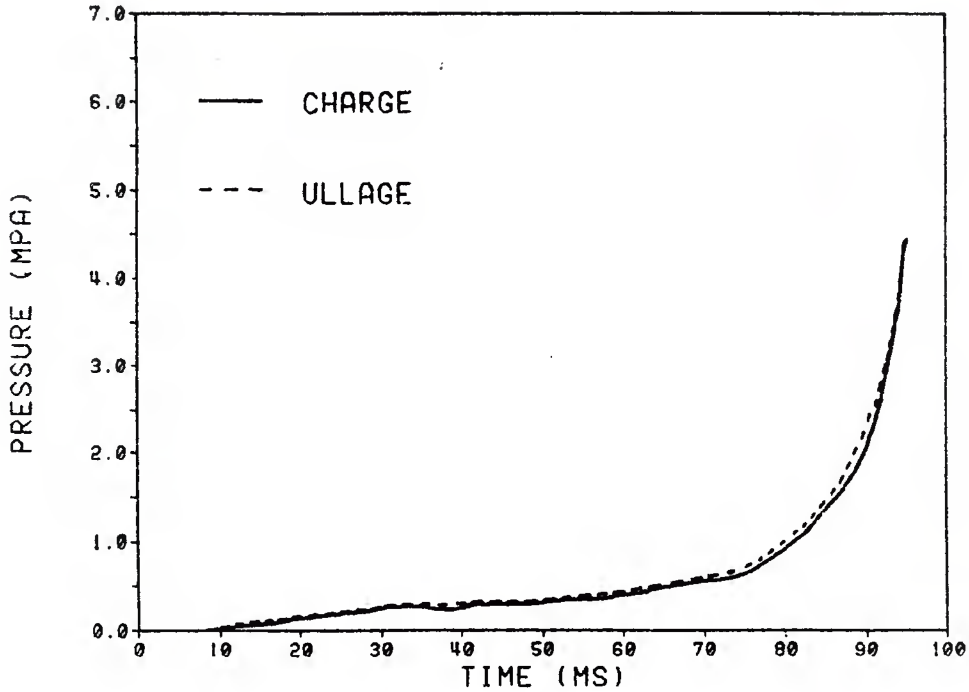

Figure 20. Pressures in Charge and Ullage, M203 Round 1, Fabric Region

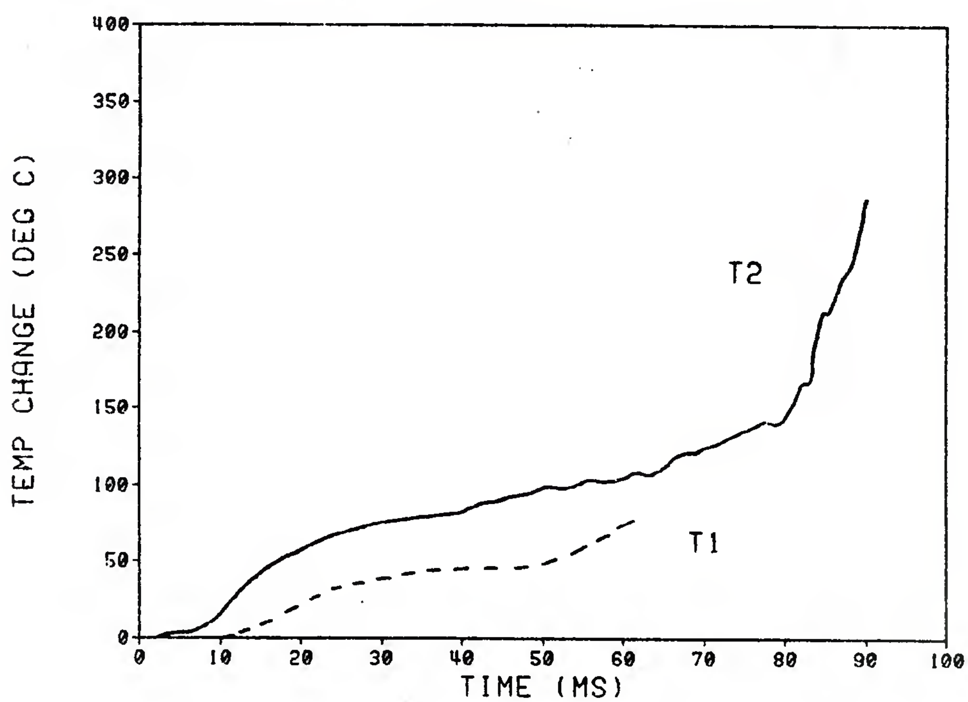

Figure 21. Propellant Grain Temperatures, M203 Round 1, 25 mm From Base

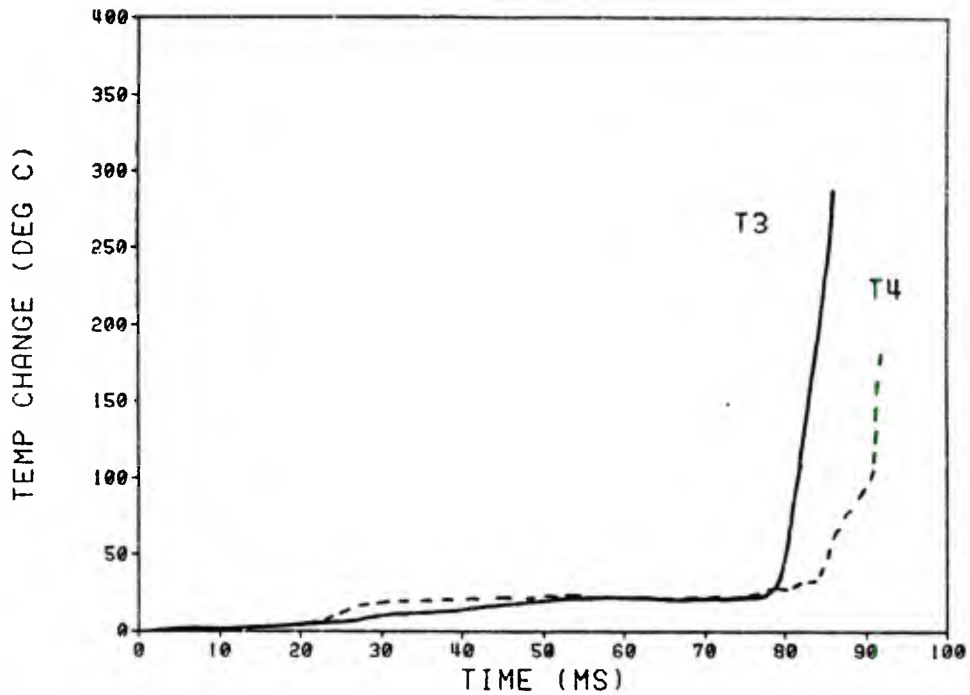

Figure 22. Propellant Grain Temperatures, M203 Round 1, 203 mm From Base

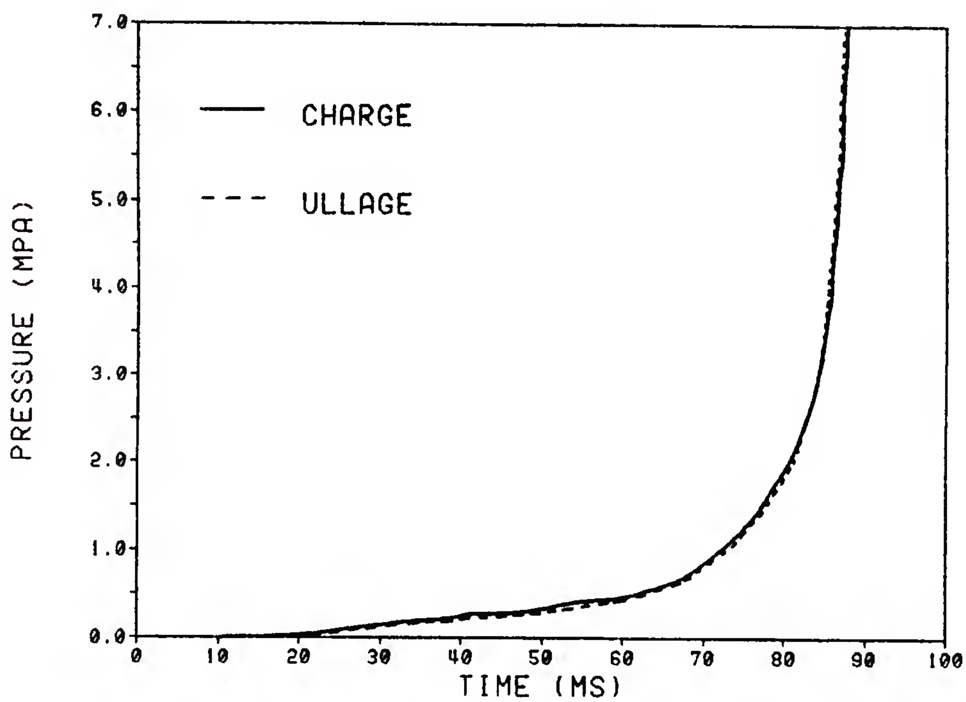

Figure 23. Pressures in Charge and Ullage, M203 Round 2, Parasitic Region

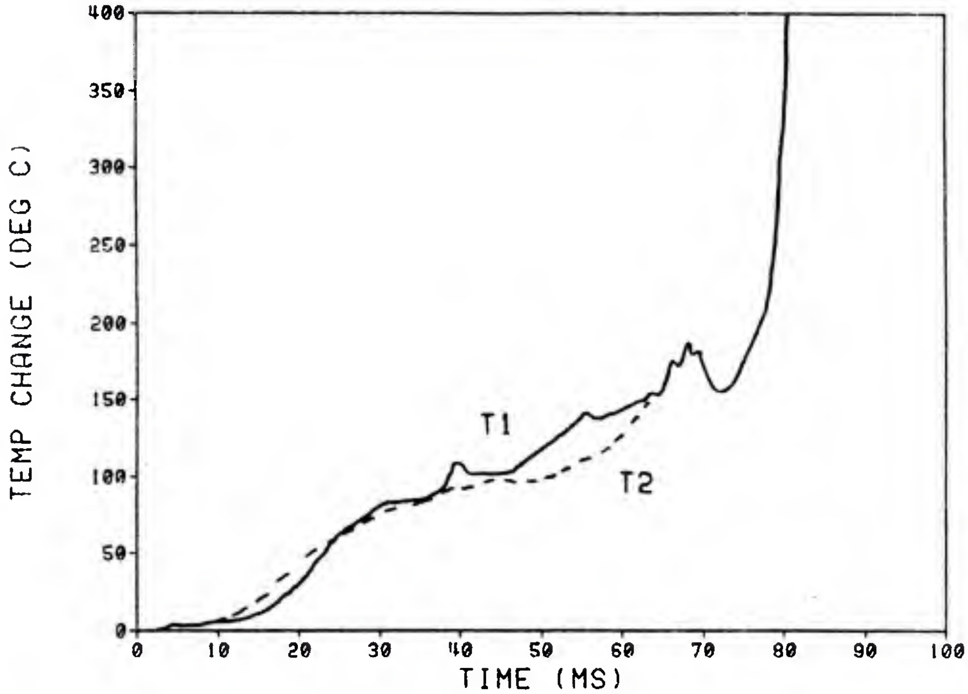

Figure 24. Propellant Grain Temperatures, M203 Round 2, 25 mm From Base

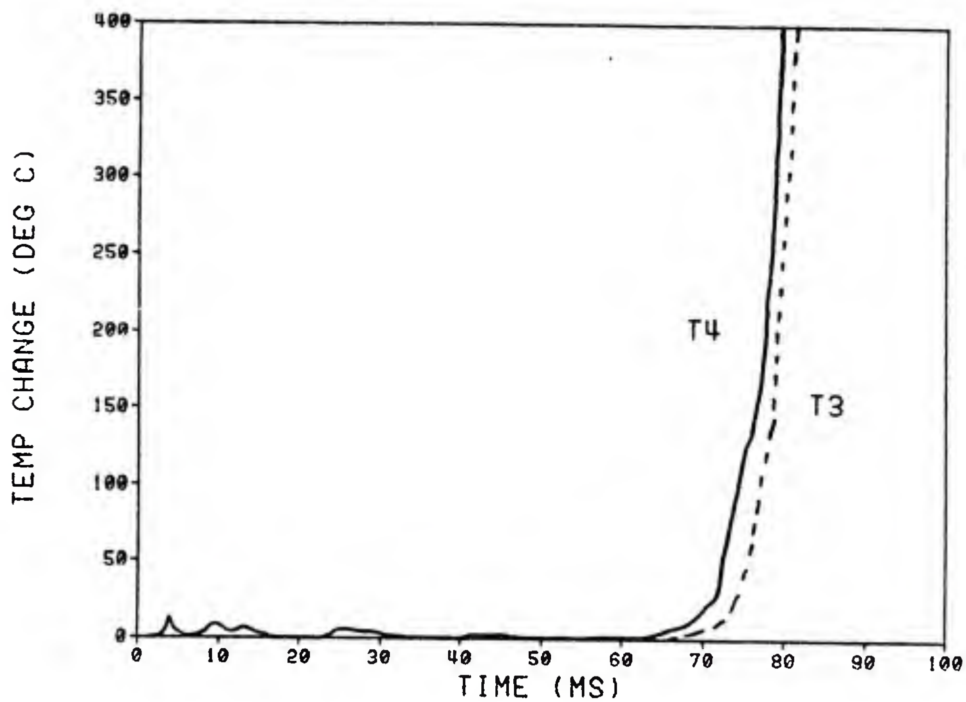

Figure 25. Propellant Grain Temperatures, M203 Round 2, 381 mm From Base

The thermocouple toward the center of the charge, T2, responded about 8 ms sooner than did that located at the charge periphery. Presumably, this difference was due to the output of the basepad impinging on T2 but not T1, since the basepad does not cover the entire rear face of the charge. There was a marked change in slope of T2 at a temperature change of approximately 135°C, which may indicate combustion of the grain. Figure 22 displays the temperature records axially farther into the charge. While there was some early heating of the propellant at 20-30 ms into the cycle, significant response on T3 and T4 was not seen until 80-90 ms. This delay was probably due to the length of time it took for the centercore to function. The usual ignition delay time for this charge lot is on the order of 40-50 ms, and indeed, we previously reported[3] the detailed functioning of each component in the igniter train as consistent with this time. The somewhat extended ignition delay is difficult to understand. It should be pointed out, though, that ignition delays on the order of 80-90 ms for M203 charges are not rare. That substantial response was seen on the T3 trace before the T4 record is not surprising, since the T3 gage was on the fabric wall and was subjected to heating from gases in the ullage before the centercore functioned, as is probably reflected in the T4 response.

Figure 23 compares the pressure measured in the ullage with that measured in the propellant bed at a location surrounded by fabric, lead and wear-reducing liners. The responses were even more nearly identical here; an examination of the digital record shows no disagreement of more than 0.10 MPa until the chamber failed at about 7 MPa. Intuitively, this is an even more surprising result than that obtained with M203 Round 1. One might perhaps expect the parasitics surrounding the charge to induce a pressure gradient between the bed and the ullage. Again, two-phase flow interior ballistic calculations corroborate this result.[4,5] In this pressure regime, the cooler initial gases are displaced from the area of burning propellant by the hotter combustion gases, so that while a gas-temperature gradient is formed between the two regions, the pressures in these regions rise at the same rate.

Figure 24 displays the measured propellant grain surface temperatures near the base of the charge, and Figure 25 shows temperatures much farther forward (381 mm from the base). As before, we note a response on T2 first, but there was also a very fast response on T1, with a delay between the two of only about 3 ms. The vagaries of the functioning of the charge supplied sufficient hot gases in the ullage in this region to produce a substantial heat flux to this grain. We note in Figure 25 that there was again a significant delay before response of the downstream thermocouples, and the previous comments on the magnitude of the delay apply here. There is one significant difference here, however. Previously the gage on the fabric periphery responded before the more centrally located thermocouple, but in this case there was a response of the inner thermocouple before that on the periphery. This should not be surprising since the T3 thermocouple is protected from hot gases in the ullage by the parasitic components surrounding the charge.

IV. CONCLUSIONS

In this paper we have presented several aspects of the multidimensional, multiregional nature of the interior ballistic cycle. Summarized, they are:

a. The clear superiority of stick propellant compared to granular propellant in permitting passage of igniter and early propellant combustion gases through the charge, thus leading to more uniform charge ignition, was demonstrated. It was also shown that the solid-phase movement was considerably more pronounced with the granular propellant, though there was evidence that the stick propellant did move.

b. Major effects of igniter material and oxygen on low-pressure, gas-phase combustion were graphically portrayed.

c. The separation of a forward increment from a multizone charge, and propulsion of that package toward the projectile, were found to be variable. Such motion was not seen in these tests, though it was observed previously with similar charges.

d. No significant differences (greater than 0.10 - 0.15 MPa) were found between the pressures inside the packed bed of axisymmetrically loaded M203-type charges and those in the ullage surrounding the charges.

e. The dependence of propellant heating on location within an axisymmetrically loaded M203-type propelling charge was shown, and the effect of surrounding charge parasitic components was noted.

The advent of multidimensional, two-phase flow models requires more well-instrumented firings to obtain data of the type discussed here, particularly that developed with the M203 charge. Future work at the BRL will concentrate on measurements of flamespread, radial and axial pressure dependence, and solid-phase dynamics in specially built axisymmetric propelling charges.

V. ACKNOWLEDGEMENTS

As usual, Mr. A. W. Horst provided much helpful guidance and insight to the author during the work. Dr. K. J. White's expertise was heavily drawn upon for the thermal instrumentation and analysis of the multizone charge firings. Mr. H. E. Holmes also consulted on thermocouple installation. Mr. A. A. Koszoru performed some of the design and much of the fabrication of the experimental charges. Mr. Koszoru and the personnel at Range 18, Spesutie Island, Messrs. J. W. Evans, J. L. Stabile, J. E. Bowen, and J. R. Hewitt, were invaluable in the conduct of the firing program.

REFERENCES

1. A. W. Horst and T. C. Minor, "Improved Flow Dynamics in Guns Through the Use of Alternative Propellant Grain Geometries," 1980 JANNAF Propulsion Meeting, CPIA Publication 315, Vol. I, pp. 325-351, March 1980.

2. E. B. Fisher, "Continued Investigation of Early Time Propellant Charge Behavior," Report No. 6816-D-1, Calspan Corporation, Buffalo, NY, June 1981.

3. T. C. Minor, "Characterization of Ignition Systems for Bagged Artillery Charges," 17th JANNAF Combustion Meeting, CPIA Publication 329, Vol. II, pp. 45-67, November 1980.

4. P. S. Gough, "Two-Dimensional Model of the Interior Ballistics of Bag Charges," 18th JANNAF Combustion Meeting, CPIA Publication 347, Vol. II, pp. 193-199, October 1981.

5. A. W. Horst, F. W. Robbins and P. S. Gough, "A Two-Dimensional, Two-Phase Flow Simulation of Ignition, Flamespread, and Pressure-Wave Phenomena in the 155-mm Howitzer," 18th JANNAF Combustion Meeting, CPIA Publication 347, Vol. II, pp. 201-215, October 1981.

DISTRIBUTION LIST

No. Of Copies	Organization
12	Administrator Defense Technical Info Center ATTN: DTIC-DDA Cameron Station Alexandria, VA 22314
2	Office of the Under Secretary of Defense Research & Engineering ATTN: G. R. Makepeace R. Thorkildsen Washington, DC 20301
1	HQDA/SAUS-OR, D. Hardison Washington, DC 20301
1	HQDA/DAMA-ZA Washington, DC 20310
2	HQDA, DAMA-CSM, LTC A. German E. Lippi Washington, DC 20310
1	HQDA/SARDA Washington, DC 20310
1	Commandant US Army War College ATTN: Library-FF229 Carlisle Barracks, PA 17013
1	Ballistic Missile Defense Advanced Technology Center P. O. Box 1500 Huntsville, AL 35804
1	Chairman DOD Explosives Safety Board Room 856-C Hoffman Bldg. 1 2461 Eisenhower Avenue Alexandria, VA 22331
3	Commander US Army Materiel Development and Readiness Command ATTN: DRCDMD-ST DCRSF-E, Safety Office DRCDE-DW 5001 Eisenhower Avenue Alexandria, VA 22333
13	Commander US Army Armament R&D Command ATTN: DRDAR-TSS DRDAR-TDC D. Gyorog DRDAR-LCA K. Russell J. Lannon A. Beardell D. Downs S. Einstein L. Schlosberg S. Westley S. Bernstein P. Kemmey C. Heyman Dover, NJ 07801
9	US Army Armament R&D Command ATTN: DRDAR-SCA, L. Stiefel B. Brodman DRDAR-LCB-I, D. Spring DRDAR-LCE, R. Walker DRDAR-LCU-CT E. Barrieres R. Davitt DRDAR-LCU-CV C.Mandala E. Moore DRDAR-LCM-E S. Kaplowitz Dover, NJ 07801

DISTRIBUTION LIST

No. Of Copies	Organization
5	Commander US Army Armament R&D Command ATTN: DRDAR-QAR, J. Rutkowski G. Allen J. Donner P. Serao D. Adams Dover, NJ 07801
7	Project Manager Cannon Artillery Weapons System ATTN: DRCPM-CAWS F. Menke (3 cys) DRCPM-CAWS-WS H. Noble DRCPM-CAWS-SI M. Fisette DRCPM-CAWS-AM R. DeKleine H. Hassmann Dover, NJ 07801
3	Project Manager Munitions Production Base Modernization and Expansion ATTN: DRCPM-PMB, J. Ziegler M. Lohr A. Siklosi Dover, NJ 07801
3	Project Manager Tank Main Armament System ATTN: DRCPM-TMA, D. Appling DRCPM-TMA-105 DRCPM-TMA-120 Dover, NJ 07801
4	Commander US Army Armament R&D Command ATTN: DRDAR-LCW-A M.Salsbury DRDAR-LCS DRDAR-LCU, A. Moss DRDAR-LC, J. Frasier Dover, NJ 07801
5	Commander US Army Armament Materiel Readiness Command ATTN: DRSAR-LEP-L DRSAR-LC, L. Ambrosini DRSAR-IRC, G. Cowan DRSAR-LEM, W. Fortune R. Zastrow Rock Island, IL 61299
1	Commander US Army Watervliet Arsenal ATTN: SARWV-RD, R. Thierry Watervliet, NY 12189
1	Director US Army ARRADCOM Benet Weapons Laboratory ATTN: DRDAR-LCB-TL Watervliet, NY 12189
1	Commander US Army Aviation Research and Development Command ATTN: DRDAV-E 4300 Goodfellow Blvd. St. Louis, MO 63120
1	Commander US Army Mobility Equipment Command 4300 Goodfellow Blvd. St. Louis, MO 63120
1	Director US Army Air Mobility Research And Development Laboratory Ames Research Center Moffett Field, CA 94035

DISTRIBUTION LIST

No. Of Copies	Organization
1	Commander US Army Communications Research and Development Command ATTN: DRSEL-ATDD Fort Monmouth, NJ 07703
1	Commander US Army Electronics Research and Development Command Technical Support Activity ATTN: DELSD-L Fort Monmouth, NJ 07703
1	Commander US Army Harry Diamond Lab. ATTN: DELHD-TA-L 2800 Powder Mill Road Adelphi, MD 20783
2	Commander US Army Missile Command ATTN: DRSMI-R DRSMI-YDL Redstone Arsenal, AL 35898
1	Commander US Army Natick Research and Development Command ATTN: DRDNA-DT, D. Sieling Natick, MA 01762
1	Commander US Army Tank Automotive Command ATTN: DRDTA-UL Warren, MI 48090
1	US Army Tank Automotive Materiel Readiness Command ATTN: DRSTA-CG Warren, MI 48090

No. Of Copies	Organization
1	Project Manager Improved TOW Vehicle ATTN: DRCPM-ITV US Army Tank Automotive Command Warren, MI 48090
1	Program Manager M1 Tank System ATTN: DRCPM-GMC-SA Warren, MI 48090
1	Project Manager Fighting Vehicle Systems ATTN: DRCPM-FVS Warren, MI 48090
1	Director US Army TRADOC Systems Analysis Activity ATTN: ATAA-SL White Sands Missile Range NM 88002
1	Project Manager M-60 Tank Development ATTN: DRCPM-M60TD Warren, MI 48090
1	Commander US Army Training & Doctrine Command ATTN: ATCD-A/MAJ Williams Fort Monroe, VA 23651
2	Commander US Army Materials and Mechanics Research Center ATTN: DRXMR-ATL Tech Library Watertown, MA 02172
2	Commandant US Army Infantry School ATTN: ATSH-CD-CSO-OR Fort Benning, GA 31905

DISTRIBUTION LIST

No. Of Copies	Organization
1	Commander US Army Research Office ATTN: Tech Library P. O. Box 12211 Research Triangle Park, NC 27709
1	Commander US Army Mobility Equipment Research & Development Command ATTN: DRDME-WC Fort Belvoir, VA 22060
1	Commander US Army Logistics Mgmt Ctr Defense Logistics Studies Fort Lee, VA 23801
2	Commandant US Army Infantry School ATTN: Infantry Agency Fort Benning, GA 31905
1	US Army Armor & Engineer Board ATTN: STEBB-AD-S Fort Knox, KY 40121
1	Commandant US Army Aviation School ATTN: Aviation Agency Fort Rucker, AL 36360
1	Commandant Command and General Staff College Fort Leavenworth, KS 66027
1	Commandant US Army Special Warfare School ATTN: Rev & Tng Lit Div Fort Bragg, NC 28307
1	Commandant US Army Engineer School ATTN: ATSE-CD Ft. Belvoir, VA 22060
1	Commander US Army Foreign Science & Technology Center ATTN: DRXST-MC-3 220 Seventh Street, NE Charlottesville, VA 22901
1	President US Army Artillery Board Ft. Sill, OK 73504
2	Commandant US Army Field Artillery School ATTN: ATSF-CO-MW, B. Willis Ft. Sill, OK 73503
3	Commandant US Army Armor School ATTN: ATZK-CD-MS/M. Falkovitch/Armor Agency Fort Knox, KY 40120
1	Chief of Naval Materiel Department of the Navy ATTN: Dr. J. Amlie Washington, DC 20360
1	Chief Naval Research ATTN: Code 473, R. S. Miller 800 N. Quincy Street Arlington, VA 22217
2	Commander Naval Sea Systems Command ATTN: SEA-62R, J. W. Murrin R. Beauregard National Center, Bldg. 2 Room 6E08 Washington, DC 20362
1	Commander Naval Air Systems Command ATTN: NAIR-954-Tech Lib Washington, DC 20360

DISTRIBUTION LIST

No. Of Copies	Organization
1	Strategic Systems Project Office Dept. of the Navy Room 901 ATTN: Dr. J. F. Kincaid Washington, DC 20376
1	Assistant Secretary of the Navy (R, E, and S) ATTN: Dr. R. Reichenbach Room 5E787 Pentagon Bldg. Washington, DC 20350
1	Naval Research Lab Tech Library Washington, DC 20375
5	Commander Naval Surface Weapons Center ATTN: Code G33, J. L. East D. McClure W. Burrell J. Johndrow Code DX-21 Tech Lib Dahlgren, VA 22448
2	Commander US Naval Surface Weapons Center ATTN: J. P. Consaga C. Gotzmer Indian Head, MD 20640
4	Commander Naval Surface Weapons Center ATTN: S. Jacobs/Code 240 Code 730 K. Kim/Code R-13 R. Bernecker Silver Spring, MD 20910
2	Commanding Officer Naval Underwater Systems Center Energy Conversion Dept. ATTN: CODE 5B331, R. S. Lazar Tech Lib Newport, RI 02840
4	Commander Naval Weapons Center ATTN: Code 388, R. L. Derr C. F. Price T. Boggs Info. Sci. Div. China Lake, CA 93555
2	Superintendent Naval Postgraduate School Dept. of Mechanical Engineering ATTN: A. E. Fuhs Code 1424 Library Monterey, CA 93940
6	Commander Naval Ordnance Station ATTN: P. L. Stang C. Smith S. Mitchell C. Christensen D. Brooks Tech Library Indian Head, MD 20640
1	AFSC/SDOA Andrews AFB Washington, DC 20334
1	Program Manager AFOSR Directorate of Aerospace Sciences ATTN: L. H. Caveny Bolling AFB, DC 20332
6	AFRPL (DYSC) ATTN: D. George J. N. Levine B. Goshgarian D. Thrasher N. Vander Hyde Tech Library Edwards AFB, CA 93523

DISTRIBUTION LIST

No. Of Copies	Organization
1	AFFTC ATTN: SSD-Tech LIb Edwards AFB, CA 93523
1	AFATL ATTN: DLYV Eglin AFB, FL 32542
1	AFATL/DLDL ATTN: O. K. Heiney Eglin AFB, FL 32542
1	ADTC ATTN: DLODL Tech Lib Eglin AFB, FL 32542
1	AFFDL ATTN: TST-Lib Wright-Patterson AFB, OH 45433
1	NASA HQ 600 Independence Avenue, SW ATTN: Code JM6, Tech Lib. Washington, DC 20546
1	NASA/Lyndon B. Johnson Space Center ATTN: NHS-22, Library Section Houston, TX 77058
1	Aerodyne Research, Inc. Bedford Research Park ATTN: V. Yousefian Bedford, MA 01730
1	Aerojet Solid Propulsion Co. ATTN: P. Micheli Sacramento, CA 95813
1	Atlantic Research Corporation ATTN: M. K. King 5390 Cheorokee Avenue Alexandria, VA 22314

No. Of Copies	Organization
1	AVCO Everett Rsch Lab Div ATTN: D. Stickler 2385 Revere Beach Parkway Everett, MA 02149
2	Calspan Corporation ATTN: E. B. Fisher Tech Library P. O. Box 400 Buffalo, NY 14225
1	Foster Miller Associates ATTN: A. Erickson 135 Second Avenue Waltham, MD 02154
1	Hercules, Inc. Bacchus Works ATTN: K. P. McCarty Magna, UT 84044
1	General Applied Science Labs ATTN: J. Erdos Merrick & Stewart Avenues Westbury Long Island, NY 11590
1	General Electric Company Armament Systems Dept. ATTN: M. J. Bulman, Room 1311 Lakeside Avenue Burlington, VT 05412
1	Hercules, Inc. Allegheny Ballistics Laboratory ATTN: R. B. Miller P. O. Box 210 Cumberland, MD 21501

DISTRIBUTION LIST

No. Of Copies	Organization
1	Hercules, Inc. Eglin Operations AFATL DLDL ATTN: R. L. Simmons Eglin AFB, FL 32542
1	IITRI ATTN: M. J. Klein 10 W. 35th Street Chicago, IL 60615
2	Lawrence Livermore Laboratory ATTN: M. S. L-355, A. Buckingham Dr. M. Finger P. O. Box 808 Livermore, CA 94550
1	Olin Corporation Badger Army Ammunition Plant ATTN: R. J. Thiede Baraboo, WI 53913
1	Olin Corporation Smokeless Powder Operations ATTN: R. L.Cook P. O. Box 222 ST. Marks, FL 32355
1	Paul Gough Associates, Inc. ATTN: P. S. Gough P. O. Box 1614 Portsmouth, NH 03801
1	Physics International Company 2700 Merced Street Leandro, CA 94577
1	Princeton Combustion Research Lab., Inc. ATTN: M. Summerfield 1041 US Highway One North Princeton, NJ 08540
1	Pulsepower Systems, Inc. ATTN: L. C. Elmore 815 American Street San Carlos, CA 94070

No. Of Copies	Organization
2	Rockwell International Corporation Rocketdyne Division ATTN: BA08 J. E. Flanagan J. Grey 6633 Canoga Avenue Canoga Park, CA 91304
1	Science Applications, INC. ATTN: R. B.Edelman 23146 Cumorah Crest Woodland Hills, CA 91364
1	Scientific Research Assoc., Inc. ATTN: H. McDonald P. O. Box 498 Glastonbury, CT 06033
1	Shock Hydrodynamics, Inc. ATTN: W. H. Andersen 4710-16 Vineland Avenue North Hollywood, CA 91602
3	Thiokol Corporation Huntsville Division ATTN: D. Flanigan R. Glick Tech Library Huntsville, AL 35807
2	Thiokol Corporation Wasatch Division ATTN: J. Peterson Tech Library P. O. Box 524 Brigham City, UT 84302
2	Thiokol Corporation Elkton Division ATTN: R. Biddle Tech Lib. P. O. Box 241 Elkton, MD 21921

DISTRIBUTION LIST

No. Of Copies	Organization
2	United Technologies Chemical Systems Division ATTN: R. Brown Tech Library P. O. Box 358 Sunnyvale, CA 94086
1	Universal Propulsion Company ATTN: H. J. McSpadden Black Canyon Stage 1, Box 1140 Phoenix, AZ 85029
1	Southwest Research Institute Institute Scientists ATTN: W. H. McLain 8500 Culebra Road San Antonio, TX 78228
1	Battelle Memorial Institute ATTN: Tech Library 505 King Avenue Columbus, OH 43201
1	Brigham Young University Dept. of Chemical Engineering ATTN: M. Beckstead Provo, UT 84601
1	California Institute of Tech 204 Karman Lab Main Stop 301-46 ATTN: F. E. C. Culick 1201 E. California Street Pasadena, CA 91125
1	California Institute of Tech Jet Propulsion Laboratory 4800 Oak Grove Drive Pasadena, CA 91103
1	University of Illinois Dept of Mech Engineering ATTN: H. Krier 144 MEB, 1206 W. Green Street Urbana, IL 61801
1	University of Massachusetts Dept. of Mechanical Engineering ATTN: K. Jakus Amherst, MA 01002
1	University of Minnesota Dept. of Mechanical Engineering ATTN: E. Fletcher Minneapolis, MN 55455
1	Case Western Reserve University Division of Aerospace Sciences ATTN: J. Tien Cleveland, OH 44135
3	Georgia Institute of Tech School of Aerospace Eng. ATTN: B. T. Zinn E. Price W. C. Strahle Atlanta, GA 30332
1	Institute of Gas Technology ATTN: D. Gidaspow 3424 S. State Street Chicago, IL 60616
1	Johns Hopkins University Applied Physics Laboratory Chemical Proplsion Information Agency ATTN: T. Christian Johns Hopkins Road Laurel, MD 20707
1	Massachusetts Institute of Tech Dept of Mechanical Engineering ATTN: T. Toong Cambridge, MA 02139

DISTRIBUTION LIST

No. Of Copies	Organization
1	Pennsylvania State University Applied Research Lab ATTN: G. M. Faeth P. O. Box 30 State College, PA 16801
1	Pennsylvania State University Dept. Of Mechanical Engineering ATTN: K. Kuo University Park, PA 16802
1	Purdue University School of Mechanical Engineering ATTN: J. R. Osborn TSPC Chaffee Hall West Lafayette, IN 47906
1	Rensselaer Polytechnic Inst. Department of Mathematics Troy, NY 12181
1	Rutgers University Dept. of Mechanical and Aerospace Engineering ATTN: S. Temkin University Heights Campus New Brunswick, NJ 08903
1	SRI International Propulsion Sciences Division ATTN: Tech Library 333 Ravenswood Avenue Menlo Park, CA 94025
1	Stevens Institute of Technology Davidson Laboratory ATTN: R. McAlevy, III Hoboken, NJ 07030
2	Los Alamos Scientific Lab ATTN: T. D. Butler, MS B216 M. Division, B. Craig P. O. Box 1663 Los Alamos, NM 87545

No. Of Copies	Organization
1	University of Southern California Mechanical Engineering Dept. ATTN: OHE200, M. Gerstein Los Angeles, CA 90007
2	University of Utah Dept. of Chemical Engineering ATTN: A. Baer G. Flandro Salt Lake City, UT 84112
1	Washington State University Dept. of Mechanical Engineering ATTN: C. T. Crowe Pullman, WA 99163

Aberdeen Proving Ground

Dir, USAMSAA
ATTN: DRXSY-D
DRXSY-MP, H. Cohen
Cdr, USATECOM
ATTN: DRSTE-TO-F
STEAP-MT, S. Walton
G. Rice
D. Lacey
C. Herud
Dir, HEL
ATTN: J. Weisz
Dir, USACSL, Bldg. E3516, EA
ATTN: DRDAR-CLB-P A
DRDAR-CLN
DRDAR-CLJ-L

USER EVALUATION OF REPORT

Please take a few minutes to answer the questions below; tear out this sheet, fold as indicated, staple or tape closed, and place in the mail. Your comments will provide us with information for improving future reports.

1. BRL Report Number ______________________

2. Does this report satisfy a need? (Comment on purpose, related project, or other area of interest for which report will be used.)

____

____

____

3. How, specifically, is the report being used? (Information source, design data or procedure, management procedure, source of ideas, etc.) ______________________

____

____

4. Has the information in this report led to any quantitative savings as far as man-hours/contract dollars saved, operating costs avoided, efficiencies achieved, etc.? If so, please elaborate.

____

____

5. General Comments (Indicate what you think should be changed to make this report and future reports of this type more responsive to your needs, more usable, improve readability, etc.) ______________________

____

____

____

6. If you would like to be contacted by the personnel who prepared this report to raise specific questions or discuss the topic, please fill in the following information.

Name: ______________________

Telephone Number: ______________________

Organization Address: ______________________

____

____